

Heterodinuclear Zn(II)-Fe(III) and Homodinuclear M(II)-M(II) [M = Zn and Ni] complexes of a Bicompartmental [NO] ligand as synthetic mimics of the hydrolase family of enzymes

Chandni Pathak, Dharmendra Kumar, Manoj Kumar Gangwar, Darshan Mhatre, Thierry Roisnel, Prasenjit Ghosh

▶ **To cite this version:**

Chandni Pathak, Dharmendra Kumar, Manoj Kumar Gangwar, Darshan Mhatre, Thierry Roisnel, et al.. Heterodinuclear Zn(II)-Fe(III) and Homodinuclear M(II)-M(II) [M = Zn and Ni] complexes of a Bicompartmental [NO] ligand as synthetic mimics of the hydrolase family of enzymes. Journal of Inorganic Biochemistry, 2018, 185, pp.30-42. 10.1016/j.jinorgbio.2018.04.018 . hal-01807874

HAL Id: hal-01807874

https://univ-rennes.hal.science/hal-01807874

Submitted on 6 Jul 2018

HAL is a multi-disciplinary open access archive for the deposit and dissemination of scientific research documents, whether they are published or not. The documents may come from teaching and research institutions in France or abroad, or from public or private research centers.

L'archive ouverte pluridisciplinaire **HAL**, est destinée au dépôt et à la diffusion de documents scientifiques de niveau recherche, publiés ou non, émanant des établissements d'enseignement et de recherche français ou étrangers, des laboratoires publics ou privés.

ACCEPTED MANUSCRIPT

Heterodinuclear Zn(II)−Fe(III) and Homodinuclear M(II)−M(II) [M = Zn and Ni] Complexes of a Bicompartmental [N_6O] Ligand as Synthetic Mimics of the Hydrolase Family of Enzymes

Chandni Pathak,[†] Dharmendra Kumar,[†] Manoj Kumar Gangwar,[†] Darshan Mhatre,[†] Thierry Roisnel,[$] and Prasenjit Ghosh*[,†]

[†]Department of Chemistry

Indian Institute of Technology Bombay

Powai, Mumbai 400 076

India

[$]Institut des Sciences Chimiques de Rennes,

Campus de Beaulieu, 263 av. du Général Leclerc,
35042 Rennes Cedex,
France

Email: pghosh@chem.iitb.ac.in

Fax: +91 22 2572 3480

ACCEPTED MANUSCRIPT

Keywords: heterodinuclear complex • homodinuclear complex • magnetic properties • small molecule enzyme models • hydrolase family of enzymes

ACCEPTED MANUSCRIPT

ACCEPTED MANUSCRIPT

Highlights

- Hetero and homodinuclear complexes of Fe, Zn and Ni act as functional mimics of hydrolases.
- Mass spectrometric detection of catalytically active monoaquated and dihydroxo species.
- Mass spectrometric detection of catalyst-substrate species in phosphodiester hydrolysis.

ACCEPTED MANUSCRIPT

ACCEPTED MANUSCRIPT

Abstract: Heterodinuclear mixed valence [Zn(II)−Fe(III)] and the homodinuclear [Zn(II)−Zn(II)] and [Ni(II)−Ni(II)] complexes of a bicompartmental ligand containing a bridging phenoxy as a O−donor and four pyridyl moieties and two amine moieties as the N−donors exhibit phosphoester hydrolysis activity similar to the hydrolase family of enzymes. While the heterodinuclear [Zn(II)−Fe(III)] (**2**) complex was obtained by the sequential addition of $Fe(NO_3)_3$•$9H_2O$ and $Zn(OAc)_2$•$2H_2O$ to the ligand 2,6-*bis*{[*bis*(2-pyridylmethyl)amino]methyl}-4-*t*-butylphenol (HL) (**1**) in moderate yield of 37 %, the homodinuclear [Zn(II)−Zn(II)] (**3**) and [Ni(II)−Ni(II)] (**4**) complexes were obtained by the direct reaction of the ligand (**1**) with $Zn(OAc)_2$•$2H_2O$ and $Ni(OAc)_2$•$2H_2O$ respectively, in good to moderate yields (43–63 %). Based on the spectrophotometric titration and the mass spectrometry studies, a monoaquated and dihydroxo species **2C**, **3C** and **4C** has been identified as the catalytically active species responsible for the phosphodiester hydrolysis of the *bis*(2,4−dinitrophenyl)phosphate (2,4−BDNPP) substrate in the pH range 5.5−10.5. The kinetic studies further revealed that the homodinuclear [Ni(II)−Ni(II)] complexes (**4**) (k_{cat} = 1.26 × 10^{-2} s^{-1}) is more active by 39 times than the homodinuclear [Zn(II)−Zn(II)] complexes (**3**) (k_{cat} = 3.20 × 10^{-4} s^{-1}) and 27 times more active than the heterodinuclear [Zn(II)−Fe(III)] complex (**2**) (k_{cat} = 4.62 × 10^{-4} s^{-1}) in the phosphodiester hydrolysis activity. Significantly enough, the catalyst−substrate adduct species (**2E**, **2F** and **3F**) containing a metal bound *bis*(2,4−dinitrophenyl)phosphate has been detected by mass spectrometry for the first time.

ACCEPTED MANUSCRIPT

Introduction

Metalloenzymes participate in a wide variety of important chemical transformations in biology that are vital to life [1-4]. Metalloenzymes contaning various types of active sites [5] like, the mononuclear ones that engage in oxygen transport and storage [6, 7], and in electron transfer reactions [8-10], the dinuclear ones involve in hydrogenation [11], oxidation [12] and hydrolysis reactions [13, 14] and the polynuclear ones in electron transfer reactions [10]. Of these, the hydrolysis reaction constitutes an important domain in the area of energy generation and DNA cleavage activities [15, 16]. In this context the dinuclear metalloenzymes namely, purple acid phosphatase (PAP) and zinc phosphoesterase bear mention as they carry out the hydrolysis of phosphoester bonds [13, 16-20].

The active sites of PAP, as isolated from fungi, plants and mammals, contains M(II)–Fe(III) [M(II) = Fe, Zn, Mn] type metal core [21-27], of which the Fe(III) site is coordinated to a tyrosine, histidine, a monodentate aspartate residue and a terminal hydroxo moiety while the M(II) site is coordinated with two histidine, an asparagine residue along with a terminal water molecule, and a bridging aspartate and a hydroxo moiety [28-30]. The active site of zinc phosphoesterase as isolated from *Pseudomonas diminuta*, contains a homodinuclear [Zn(II)-Zn(II)] type metal core with one of the Zn(II) center being bound to two histidine moieties while the other Zn(II) center bound to two histidine, an aspartate residue, a bridging carbamylated lysine and a hydroxo moiety [31, 32]. The current synthetic modelling study of dinuclear active sites of the phosphoesterase enzymes also gains prominence in the context of several Organophosphate Hydrolases (OPHs) that are found in soil dwelling micro-organism [13, 33-36]. Of the several organophosphate hydrolases (OPHs) that are known, the phosphotriesterase

ACCEPTED MANUSCRIPT

(PTE) enzyme, found in *Flavobacterium* sp ATCC 27551 and *P. diminuta*, is by far the most studied one and is known to possess a homodinuclear [Zn–Zn] active site [37, 38]. Hence, in this context, the current attempt of performing biomimetic studies of the homo- and the heterodinuclear transition metal complexes assume relevance. In particular, in order to understand the role of zinc in the heterodinuclear PAP and the homodinuclear OPH enzymes, we wanted to employ other transition metal complexes including nickel in synthesizing the enzyme mimics.

Various ligands both of the symmetrical [39-49] and unsymmetrical [31, 42, 50-57] types having a variety of binucleating metal bridging sites namely {[N_3O], [N_3O]} [41-43, 58-61], {[N_3O], [N_2O_2]} [55-57, 62-70], {[N_3O], [NO_3]} [71, 72], {[N_3O], [N_2O]} [73], {[N_2O_2], [NO_3]} [52] {[N_2O_2], [N_2O]} [31, 74-79], {[N_2O_2], [N_2O_2]} [79-85], {[N_2O], [N_2O]} [86-89] and the {[NO_2], [N_3O]} [90] types have been reported in literature. In this regard, we intend to design synthetic mimics of the dinucleating enzymes namely, PAP and zinc phosphoesterase using a symmetrical ligand containing a phenoxy bridge and tetra pyridine side arms.

One of our longstanding interest remains in designing synthetic models for various types of mononuclear and dinuclear metalloenzymes, for example, catechol oxidase [91], the catechol dioxygenase [92] and the galactose oxidase [93]. In this context, we set out to design synthetic mimics of PAP and zinc phosphoesterase containing dinuclear active sites using bicompartmental ligands. In this pursuit, we have recently reported an [N_6O] type unsymmetrical ligand and its corresponding heterodinuclear M(II)–Fe(III) (M = Zn, Ni, Co and Cu) complexes as the small molecule models for the PAP enzyme [94]. To gain more insight

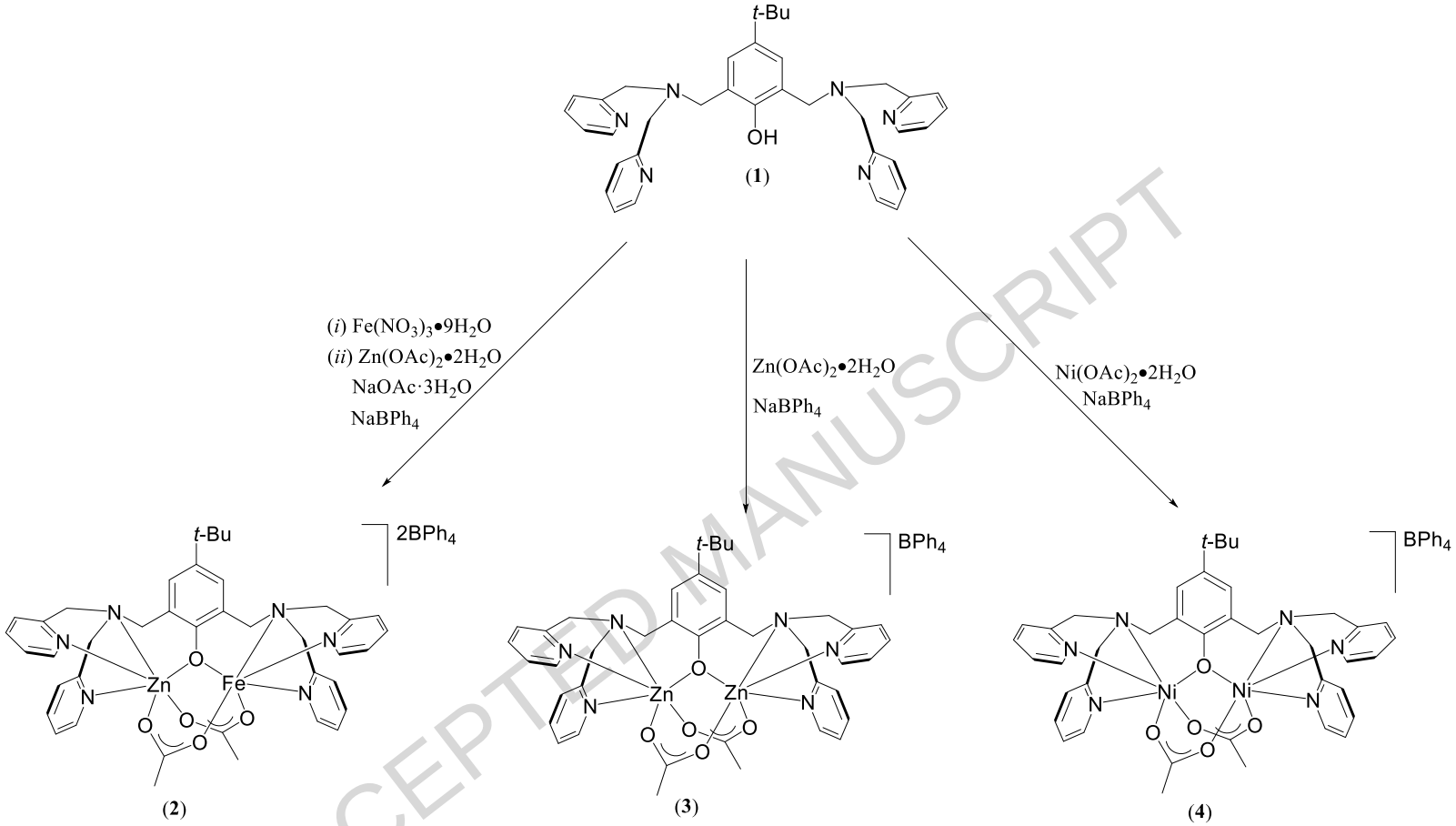
ACCEPTED MANUSCRIPT

into the nature of these types of active site models, we undertook the synthesis of symmetrical ligands and their transition metal complexes.

Here in this manuscript, we report the synthesis and structural characterization of the dinuclear $\{L[M^1(\mu\text{–}OAc)_2M^2]\}(BPh_4)_n$ {[where, M^1 = Zn(II), M^2 = Fe(III) (**2**); n = 2: $M^1 = M^2$ = Zn(II) (**3**) and Ni(II) (**4**); n = 1] and L = 2,6-*bis*{[*bis*(2-pyridylmethyl)amino]methyl}-4-*t*-butylphenoxide} complexes supported over a bicompartmental $[N_6O]$ type symmetrical ligand that serve as synthetic mimics of the active sites of PAP and the zinc phosphoesterase enzymes (Scheme 1).

ACCEPTED MANUSCRIPT

ACCEPTED MANUSCRIPT



Scheme 1. Synthesis of the the hetero- and homodinuclear complexes supported over symmetrical [N_6O] ligand **1**.

ACCEPTED MANUSCRIPT

Results and discussion

Dinuclear metal complexes

The phenoxy bridge bicompartmental [N_6O] ligand namely, 2,6-*bis*{[*bis*(2-pyridylmethyl)amino]methyl}-4-*t*-butylphenol (HL) (**1**), containing a phenoxy moiety, four pyridyl and two amine moieties, was synthesized according to the literature procedure [95]. The heterodinuclear mixed valence [Zn(II)–Fe(III)] (**2**) was prepared from the ligand by the sequential addition of the metal precursors, $Fe(NO_3)_3$•$9H_2O$ and $Zn(OAc)_2$•$2H_2O$ in the presence of NaOAc followed by the addition of $NaBPh_4$ resulting in the precipitation of the product in 37 % yield. Likewise, the homodinuclear [Zn(II)−Zn(II)] (**3**) and [Ni(II)−Ni(II)] (**4**) were prepared directly from the ligand HL (**1**) by the addition of $Zn(OAc)_2$•$2H_2O$ and $Ni(OAc)_2$•$2H_2O$ respectively, in the presence of NEt_3 as a base and subsequent precipitation of the product with $NaBPh_4$ in 43–63 % of yield (Scheme 1).

The characteristic tyrosine-to-Fe(III) charge-transfer transition that appear at *ca*. 546 nm (ε = 2000 $M^{-1}cm^{-1}$) in PAP enzyme [96, 97] could be observed in the heterodinuclear [Zn(II)–Fe(III)] (**2**) complex at 562 nm (ε = 864 $M^{-1}cm^{-1}$), similar to that observed in other related metal complexes [98, 99], along with the ligand based transitions at 225 nm and 294 nm (Table 1 and Supporting Information Figure S6–S7). Quite expectedly, the homodinuclear [Zn(II)–Zn(II)] (**3**) complex did not show the characteristic ligand-to-metal charge-transfer transition but only exhibited ligand based transitions at 220 nm, 259 nm and 306 nm (Table 1 and Supporting Information Figure S30) [59]. Similarly, the homodinuclear [Ni(II)–Ni(II)] (**4**) complex also lacks the characteristic ligand-to-metal charge-transfer transition but exhibited ligand based transitions at 215 nm, 257 nm and 311 nm along with the *d*–*d* transitions occurring at 600 nm

ACCEPTED MANUSCRIPT

and 961 nm [100, 101]. The weak absorption bands arising at 776 nm and 824 nm can be attributed to spin forbidden transitions (Table 1 and Supporting Information Figure S44–S45) [101].

The molecular structures of the heterodinuclear [Zn(II)–Fe(III)] (**2**) complex and the homodinuclear [Zn(II)−Zn(II)] (**3**) and [Ni(II)−Ni(II)] (**4**)] complexes, as determined by the X-ray single crystal diffraction studies, showed two metal centers being stabilized by a bridging phenoxide, four pyridyl and two amine moieties of the symmetrical [N_6O] ligand (**1**) in each of the three complexes (Table 4, Figure 1 and Supporting Information Figures S1–S2). The two M–O distances of the metal bound to a bridging phenoxide−O atom distances were observed to be in the range of 2.0050(12)–2.0493(12) Å and 2.0169(12)–2.040(3) Å in each of the heterodinuclear [Zn(II)–Fe(III)] (**2**) complex, and the homodinuclear [Zn(II)−Zn(II)] (**3**) and [Ni(II)−Ni(II)] (**4**)] complexes (Figure 1, Table 2 and Supporting Information Figures S1–S2). In addition, the two acetate moieties are bound unsymmetrically to each of the metal centers exhibiting unequal M–O(acetate) bond distances in the ranges of [2.005(4)–2.0217(12) Å and 1.9846(14)–2.0833(13) Å] and [2.0645(12)–2.1316(14) Å and 1.9846(14)–2.0833(13) Å] (Figure 2–4, Table 2) in the heterodinuclear [Zn(II)–Fe(III)] (**2**) and the homodinuclear [Zn(II)−Zn(II)] (**3**) and [Ni(II)−Ni(II)] (**4**)] complexes. Indeed, the IR spectroscopy further corroborated the presence of two ionic carboxylate moieties as observed from the C−O stretching bands at 1604−1606 cm^{-1} (symmetrical) and at 1424−1427 cm^{-1} (unsymmetrical) [76, 102]. Additional confirmation of the heterodinuclear [Zn(II)−Fe(III)] core in the heterodinuclear [Zn(II)–Fe(III)] (**2**) complex came from the Inductively Coupled Plasma Atomic Emission Spectroscopy

ACCEPTED MANUSCRIPT

(ICPAES) data (Supporting Information Table S1) of the [Zn(II)−Fe(III)] (**2**) complex that gave Fe (III) : Zn (II) [Fe (4.04 ppm), Zn (3.60 ppm)] in the ratio of 1:1 consistent with the X-ray data.

Of particular interest is the M•••M distance of 3.459(12) Å (Tables 2 and 3) in the heterodinuclear [Zn(II)−Fe(III)] (**2**) complex which is in agreement with the observation of 3.1 Å distance in the Fe•••Zn centers in the Red kidney bean PAP [27] and of 3.31Å distance in the Fe•••Fe center in the mammalian PAP [23, 103]. Slightly longer M•••M distance in the heterodinuclear [Zn(II)−Fe(III)] (**2**) complex [3.459(12) Å] than the PAP enzyme (3.1 Å) is possibly due to the presence of bridging acetate moieties in the heterodinuclear [Zn(II)−Fe(III)] (**2**) complex as opposed to a bridging hydroxide moiety in the PAP enzyme [23, 104], which also contain a bridged phosphate moiety [103]. Significantly enough, the M•••M distance of 3.337(11) Å in the homodinuclear [Zn(II)−Zn(II)] (**3**) complex is however comparable with the Zn•••Zn distance of 3.4 Å in the active site of zinc phosphoesterase as isolated from *Pseudomonas diminuta* bacteria [32] and 3.4–3.5 Å in active site of phosphotriesterase (PTE) in *Flavobacterium* sp ATCC 27551 [105]. Similarly, the M•••M distance of 3.3853(4) Å in the homodinuclear [Ni(II)−Ni(II)] (**4**) complex is also comparable to the M•••M distance of 3.1 Å in the Fe•••Zn centers of the Red kidney bean PAP [27] and of 3.31 Å distance in the Fe•••Fe center in the mammalian PAP [23] and also with the Zn•••Zn distance of 3.4 Å in the active site of zinc phosphoesterase as isolated from *Pseudomonas diminuta* bacteria [32]. All of the M•••M distance in the heterodinuclear [Zn(II)−Fe(III)] (**2**) complex and the homodinuclear [Zn(II)−Zn(II)] (**3**) and [Ni(II)−Ni(II)] (**4**)] complexes compared well with that of the other related structures known in the literature (Table 3).

ACCEPTED MANUSCRIPT

ACCEPTED MANUSCRIPT

ACCEPTED MANUSCRIPT

Table 1. Electronic spectral data for **2**, **3** and **4** in CH_3CN at room temperature.

S. No.	metal complex	λ_{max} (nm)	ε ($M^{-1}cm^{-1}$)	transitions
1.	**2** [Zn(II)–Fe(III)]	225	31331	
		294	5508	
		562	864	LMCT
2.	**3** [Zn(II)–Zn(II)]	220	23453	
		259	10023	
		306	2258	
3.	**4** [Ni(II)–Ni(II)]	215	143560	
		257	57120	
		311	11390	
		600	13.7	*d*–*d*
		776	6.17	
		824	7.09	
		961	14.7	*d*–*d*

ACCEPTED MANUSCRIPT

ACCEPTED MANUSCRIPT

Table 2. Geometric parameters of the in the hetero- and homodinuclear complexes (**2**–**4**).

	M•••M (Å)	M−O−M (°)	M−O (Å) (phenolate–O),	M−O (Å) (acetate–O)
{L[Zn^{II}(μ–OAc)$_2$$Fe^{III}$]}($BPh_4$)$_2$ (**2**)	3.459(12)	Fe2−O31−Zn1 115.82(6)	Zn1−O31 2.0493(12) Fe2−O31 2.0332(12)	Zn1−O2 2.0118(13), Zn1−O6 2.1316(14), Fe2−O8 1.9846(14), Fe2−O4 2.0237(14)
{L[Zn^{II}(μ–OAc)$_2$$Zn^{II}$]}$BPh_4$ (**3**)	3.337(11)	Zn1−O5−Zn2 109.99(16)	Zn1−O5 2.034(3) Zn2−O5 2.040(3)	Zn1−O1 2.112(4) Zn1−O2 2.005(4) Zn2−O3 2.026(4) Zn2−O4 2.150(4)
{L[Ni^{II}(μ–OAc)$_2$$Ni^{II}$]}$BPh_4$ (**4**)	3.3853(4)	Ni1−O3−Ni2 114.65(6)	Ni1−O3 2.0050(12) Ni2−O3 2.0169(12)	Ni1−O1 2.0645(12) Ni2−O2 2.0217(13) Ni1−O4 2.0217(12) Ni2−O5 2.0833(13)

ACCEPTED MANUSCRIPT

Table 3. Comparison of the M•••M distances of hetero- and homodinuclear complexes **2**–**4** with well known structurally characterized dinuclear models.

dinuclear models	dinuclear complexes [ref]	M•••M (Å)
[Zn(II)–Fe(III)]	{L[Zn^{II}(μ–OAc)$_2$$Fe^{III}$]}($BPh_4$)$_2$ (**2**) [our work]	**3.459(12)**
	[FeZnBPMP(OAc)$_2$](BPh_4)$_2$ [106]	3.437(1)
	[$Zn^{II}Fe^{III}$BPMOP{$O_2P(OPh)_2$}$_2$](ClO_4)$_2$ [44]	3.7030(7)
	{L^1[Zn^{II}(μ-OAc)$_2$$Fe^{III}$]}($ClO_4$)$_2$ [94]	3.415(12)
	[$Zn^{II}Fe^{III}$ (BMMHP)(CH_3COO)$_2$](BPh_4) [52]	3.421
	[$Zn^{II}Fe^{III}$(IPCPMP)(OAc)$_2$(CH_3OH)][PF_6] [76, 78]	3.4556(6)
	[$Zn^{II}Fe^{III}$(BPBPMP)(OAc)$_2$]ClO_4 [69]	3.490(9)
[Zn(II)–Zn(II)]	{L[Zn^{II}(μ–OAc)$_2$$Zn^{II}$]}($BPh_4$)$_2$ (**3**) [our work]	**3.337(11)**
	[Zn_2(BPMP)(OAc)$_2$]PF_6 [59]	3.3714(4)
	[Zn_2L^2OH] [107]	3.0696(13)
	[Zn_2L^2(CH_3OH)$_3$](ClO_4) [108]	3.5513(7)
	[Zn_2(TPDP)(OAc)](ClO_4)$_2$ [58]	3.465(5)
	[Zn_2(CH_3L^3)-(CH_3COO)$_2$]BPh_4 [75]	3.2391(6)
	[$Zn^{II}{}_2$(L^4)(μ-O_2CMe)$_2$($MeCN$)$_2$][BPh_4] [40]	3.3689(14)
[Ni(II)–Ni(II)]	{L[Ni^{II}(μ–OAc)$_2$$Ni^{II}$]}($BPh_4$)$_2$ (**4**) [our work]	**3.3853(4)**
	[Ni_2(OAc)$_2$(AA)(urea)(tmen)$_2$][OTf] [109]	3.434(1)
	[Ni_2(μ-L^{Cl}O)(μ$_2$-OAc)$_2$](PF_6) [100]	3.4131(5)
	[Ni_2(L^5)(OAc)$_2$(CH_3CN)]BPh_4 [110]	3.486(1)
	[Ni_2(L^6)(OAc)$_2$(CH_3CN)]BPh_4 [110]	3.431(1)
	[Ni_2(BCIMP)Ac_2]$^-$ [111]	3.396(2)
bioactive enzymes	Red kidney bean PAP (Fe•••Zn) [27]	3.1
	mammalian PAP (Fe•••Zn) [23]	3.31
	zinc phosphoesterase (isolated from *Pseudomonas diminuta* bacteria) (Zn•••Zn) [32]	3.4

Where as, HBPMP = 2,6-bis[(bis(2-pyridylmethyl)amino)methyl)]-4-methylphenol; HBPMOP = 2,6-bis[{bis(2-pyridylmethyl)amino}methyl]-4-methoxyphenol; BMMHP = 2-{[bis(2-methoxyethyl)-amino]methyl}-6-{[(2-hydroxybenzyl)(2-pyridylmethyl)amino]-methyl}-4-methylphenol; IPCPMP = 2-(N-isopropyl-N-((2-pyridyl)methyl)aminomethyl)-6-(N-(carboxylmethyl)-N-((2-pyridyl)methyl)aminomethyl)-4-methylphenol; HL^1 = 2-{[bis(2-methylpyridyl)-amino]methyl}-6-{[((1-methylimidazol-2-yl)methyl)(2-pyridylmethyl)amino]methyl}-4-t-butylphenol; H_2BPBPMP = 2-bis[{(2-pyridylmethyl)-aminomethyl}-6-{(2-hydroxybenzyl)(2-pyridylmethyl)}-aminomethyl]-4-methylphenol; H_3L^2 = 2,6-bis{[(2-hydroxybenzyl)(2-pyridylmethyl)amino]methyl]-4-methylphenol); HTPDP = 1,3-bis(bis-pyridin-2-ylmethylamino)propan-2-ol; CH_3L^3 = 2-(((2-methoxyethyl)(pyridine-2-ylmethyl)-amino)methyl)-4-methyl-6-(((pyridin-2-ylmethyl)(4-vinylbenzyl)-amino)methyl)phenol; H_3L^4 = 2,6-bis((hydroxyethyl)(methoxyethyl)-aminomethyl)-4-methylphenol; AA= acetohydroxamate anion; tmen = N,N,N′,N′-tetramethylethylenediamine; L^5 = 2-[N-bis-(2-pyridylmethyl)aminomethyl]-4-methyl-6-[N-(2-pyridylmethyl)aminomethyl]phenolate); L^{Cl}-OH = 2,6-bis[bis(2-pyridylmethyl)aminomethyl]-4-chlorophenol; L^6 = 2-[N-bis-(2-pyridylmethyl)aminomethyl]-4-methyl-6-[N-(2-pyridylmethyl)aminomethyl]phenolate); BCIMP = 2,6-bis[N-(N-(carboxylmethyl)-N-((1-methylimidazolyl)methyl)amine)methyl]-4-methylphenolate

ACCEPTED MANUSCRIPT

Table 4. X-ray crystallographic data for **2**, **3** and **4**.

Compound	**2**	**3**	**4**
Lattice	Monoclinic	Triclinic	Triclinic
Formula	$C_{88}H_{85}B_2FeN_6O_5Zn$	$C_{64}H_{65}BN_6O_5Zn_2$	$C_{64}H_{65}BN_6Ni_2O_5$
Formula weight	1449.46	1139.81	1126.45
Crystal size (mm^3)	0.43 × 0.38 × 0.25	0.259 × 0.222 × 0.184	0.193 × 0.181 × 0.149
Space group	*C*2/c	*P*-1	*P*-1
a/Å	28.6115(8)	12.690(3)	12.7077(3)
b/Å	23.2046(6)	14.626(3)	14.6050(3)
c/Å	27.3176(7)	14.882(3)	14.9200(3)
α/°	90	88.758(5)	88.6559(17)
β/°	121.9510(10)	89.849(6)	89.5428(17)
γ/°	90	88.014(5)	87.8160(18)
V/$Å^3$	15389.0(7)	2759.8(10)	2766.25(10)
Z	8	2	2
Temperature (K)	150(2)	100(2)	293(2)
Radiation (λ,Å)	0.71073	0.71073	0.71073
ρ (calcd.), g cm^{-3}	1.251	1.372	1.352
Absorption coefficient (mm^{-1})	0.557	0.926	0.738
θ range (deg.)	2.99 to 27.44	3.05 to 25.39	1.93 to 25.00
Reflections collected	68397	21737	48611
Data / restraints / parameters	17517 / 0 / 934	9918 / 468 / 703	9741 / 0 / 708
Independent reflections [R_{int}]	17517 [0.0504]	9918 [0.0533]	9741 [0.0494]
Completeness to θ = 25.000	99.7 %	97.7 %	99.9 %
Final *R* indices [I>2(*σ*)]	R1 = 0.0435, wR2 = 0.0972	R1 = 0.0505, wR2 = 0.1290	R1 = 0.0322, wR2 = 0.0756
R indices (all data)	R1 = 0.0696, wR2 = 0.1045	R1 = 0.0781, wR2 = 0.2249	R1 = 0.0377, wR2 = 0.0793
GOF	1.059	1.025	1.051
Largest diff. peak and hole ($eÅ^{-3}$)	0.341 and -0.471	1.086 and -1.500	0.392 and -0.427

ACCEPTED MANUSCRIPT

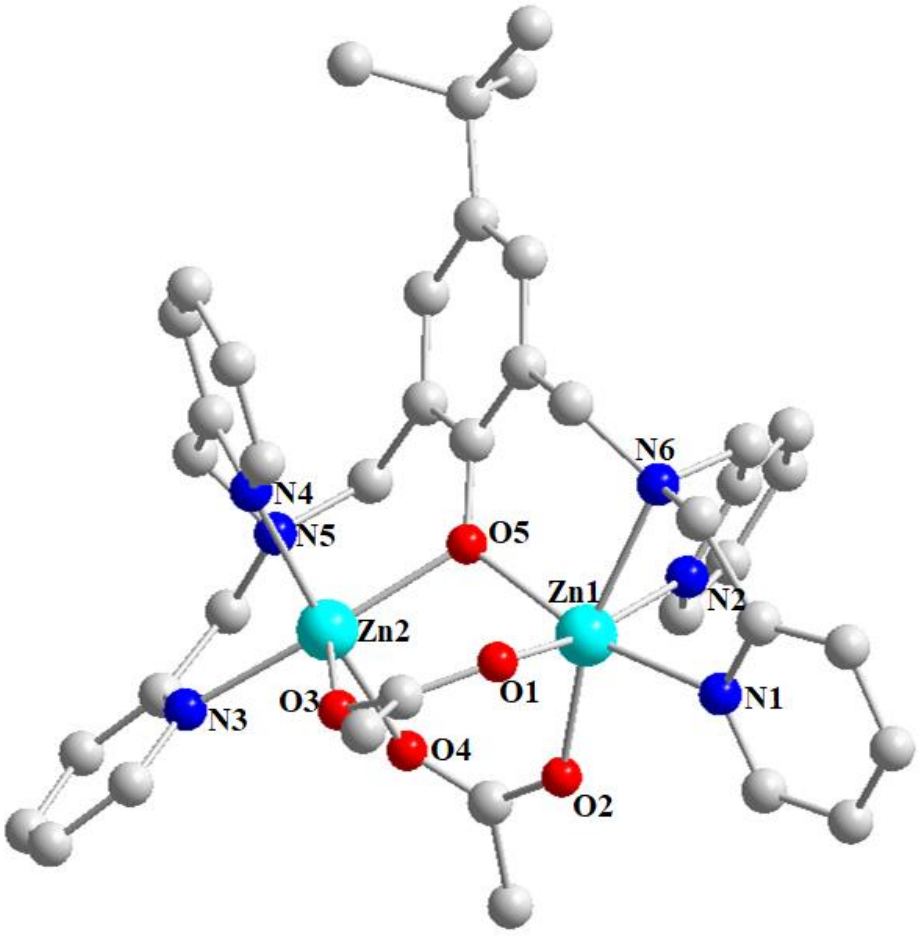


Figure 1. Perspective view of complex **3** with partial atom numbering schemes. A BPh_4^- anion has been omitted for the sake of clarity. Selected bond lengths (Å) and angles (o): Zn1−O2 2.005(4), Zn1−O5 2.034(3), Zn1−O1 2.112(4), Zn1−N1 2.157(4), Zn1−N2 2.193(4), Zn1−N6 2.251(5), Zn2−O3 2.026(4), Zn2−O5 2.040(3), Zn2−N3 2.125(4), Zn2−O4 2.150(4), Zn2−N4 2.204(5), Zn2−N5 2.207(4), Zn1−O5−Zn2 109.99(16).

ACCEPTED MANUSCRIPT

Magnetic studies

To get a closer look at the magnetic behaviour of the heterodinuclear [Zn(II)–Fe(III)] (**2**) and homodinuclear [Ni(II)–Ni(II)] (**4**) complexes, the magnetic property studies were undertaken. The variable temperature magnetic susceptibility measurements were carried out at the magnetic field of 5000 Oe in the temperature range of 4–300 K and the data were fitted using PHI software. (Figure 2 and Supporting Information Tables S2–S3 and Figures S8−S10 and S46−S48) [112].

In particular, the variable temperature magnetic susceptibility measurement for the heterodinuclear [Zn(II)–Fe(III)] (**2**) complex showed a constant $\chi_M T$ plot with a value of 4.25 cm^3mol^{-1} K at room temperature and that corresponded to an effective magnetic moment of (μ_{eff}) of 5.85 μ_B. The above results were consistent with the presence of only one magnetically active center in the form of high spin Fe(III) (S = 5/2) having five unpaired electron (μ_s = 5.9 μ_B)[113] in the [Zn(II)–Fe(III)] (**2**) complex. The fitting of the $\chi_M T$ plot using PHI software gave a g_{Fe} value of 1.99 for the Fe(III) center (Figure 2).

The homodinuclear [Ni(II)–Ni(II)] (**4**) complex with two divalent nickel centers having two unpaired electrons corresponding to an ground state of S = 1. The complex (**4**) exhibited an effective magnetic moment of 4.59 μ_B at room temperature consistent with the presence of a weak antiferromagnetic coupling between the two Ni(II) center. The confirmation of the same came from the variable temperature $\chi_M T$ plot that showed a decrease of $\chi_M T$ value with temperature due to the antiferromagnetic coupling between the two Ni(II) center (Figure 2). The

ACCEPTED MANUSCRIPT

curve fitting analysis using the PHI software gave g value of g_{Ni} = 2.00 and an exchange coupling J = −1.05 cm^{-1} comparable to the earlier observed ranges of g_{Ni} (2.17−2.18) and the exchange coupling in the range J [−(0.8−3.8) cm^{-1}] for the related dinuclear Ni(II)−Ni(II) complexes known in the literature [87, 88, 100, 113].

ACCEPTED MANUSCRIPT

ACCEPTED MANUSCRIPT

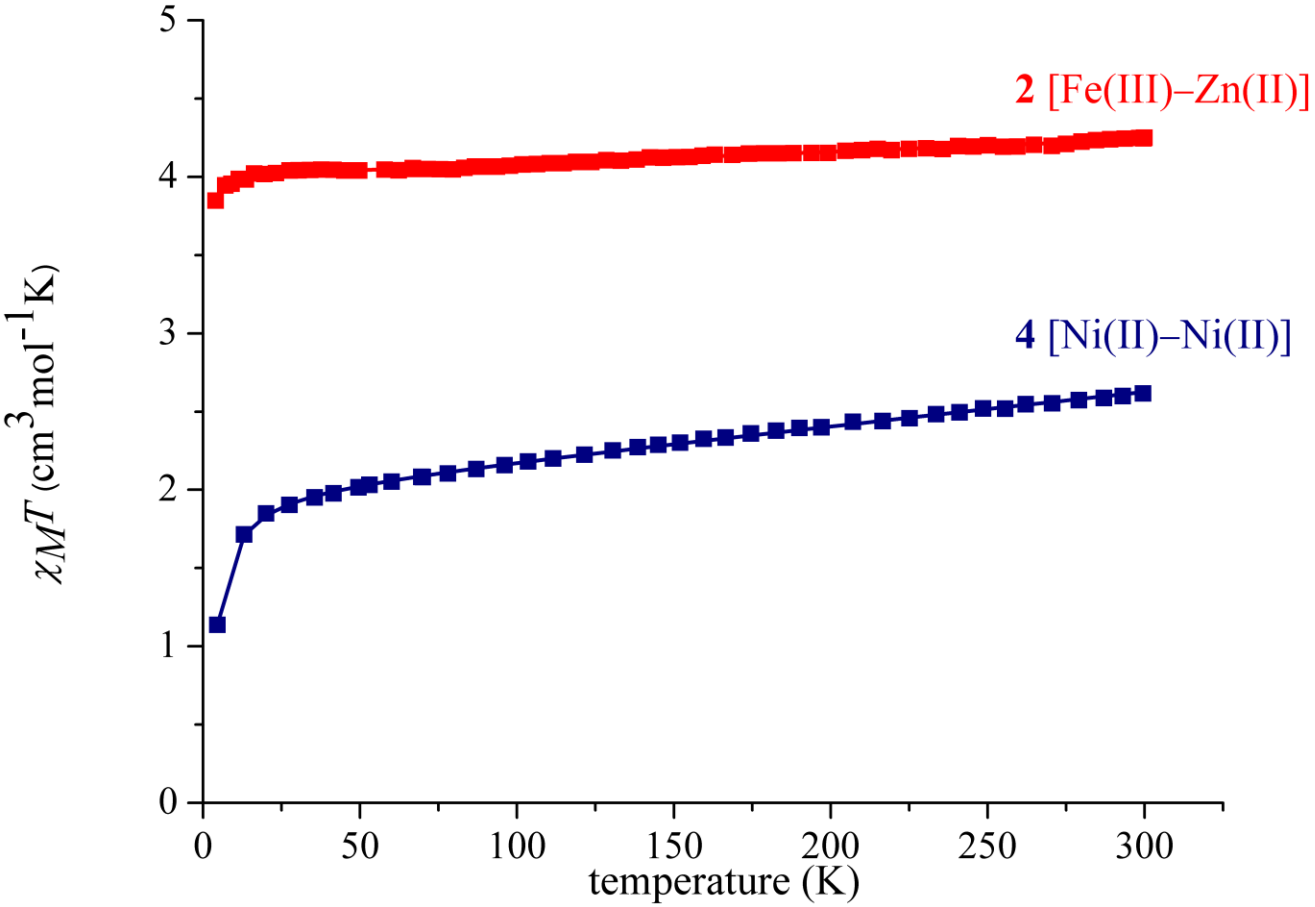


Figure 2. An overlay of variable temperature $\chi_M T$ plot of powder sample of the hetero- and homodinuclear complexes (**2** and **4**) supported over symmetrical ligand supported over symmetrical ligand **1** measured at 5000 Oe (the solid line represents the best fit curve).

ACCEPTED MANUSCRIPT

Spectrophotometric titration studies

Spectrophotometric titrations under kinetic conditions in CH_3CN/H_2O (*v/v* 1:1) undertaken at the pH range of 5.65−7.10 for the [Zn(II)–Fe(III)] (**2**) complex, at the pH range of 6.80−9.20 for the [Zn(II)–Zn(II)] (**3**) complex and at the pH range of 6.80–13.2 for the [Ni(II)–Ni(II)] (**4**) complex provided valuable insights about the various aquated species that exist in equilibrium in solution (Scheme 2, Table 5, Figure 3 and Supporting Information Tables S4−S5). In particular, the [Zn(II)–Fe(III)] (**2**) complex showed hypsochromic shift of $\Delta\lambda$ = 89 nm of the characteristic LMCT band from λ_{max} 562 nm in CH_3CN to 473 nm in CH_3CN/H_2O (*v/v* 1:1). The [Zn(II)–Zn(II)] (**3**) complex too showed similar hypsochromic shift of $\Delta\lambda$ = 11 nm of the ligand based transition from λ_{max} 306 nm in CH_3CN to 295 nm in the mixed medium of CH_3CN/H_2O (*v/v* 1:1). Similarly, the homodinuclear [Ni(II)–Ni(II)] (**4**) complex showed a hypsochromic shift of $\Delta\lambda$ = 8 nm of the ligand based transition from λ_{max} 311 nm in CH_3CN to 303 nm in the mixed medium of CH_3CN/H_2O (*v/v* 1:1). Furthermore, no change in the λ_{max} values of the remaining ligand based transitions for the heterodinuclear [Zn(II)–Fe(III)] (**2**) complex at 225 nm and 294 nm and for the homodinuclear [Zn(II)–Zn(II)] (**3**) complex at 259 nm and 220 nm were observed and for the the homodinuclear [Ni(II)–Ni(II)] (**4**) complex at 215 nm and 257 nm were observed. This results ascertain that the aquated species were formed by the replacement of bridging acetate moieties with H_2O molecules in the heterodinuclear [Zn(II)–Fe(III)] (**2**) complex and the homodinuclear [Zn(II)–Zn(II)] (**3**) and [Ni(II)–Ni(II)] (**4**) complexes.

Further evidence of the presence of different aquated species in the solution for the heterodinuclear [Zn(II)–Fe(III)] (**2**) complex and the homodinuclear [Zn(II)–Zn(II)] (**3**) and

ACCEPTED MANUSCRIPT

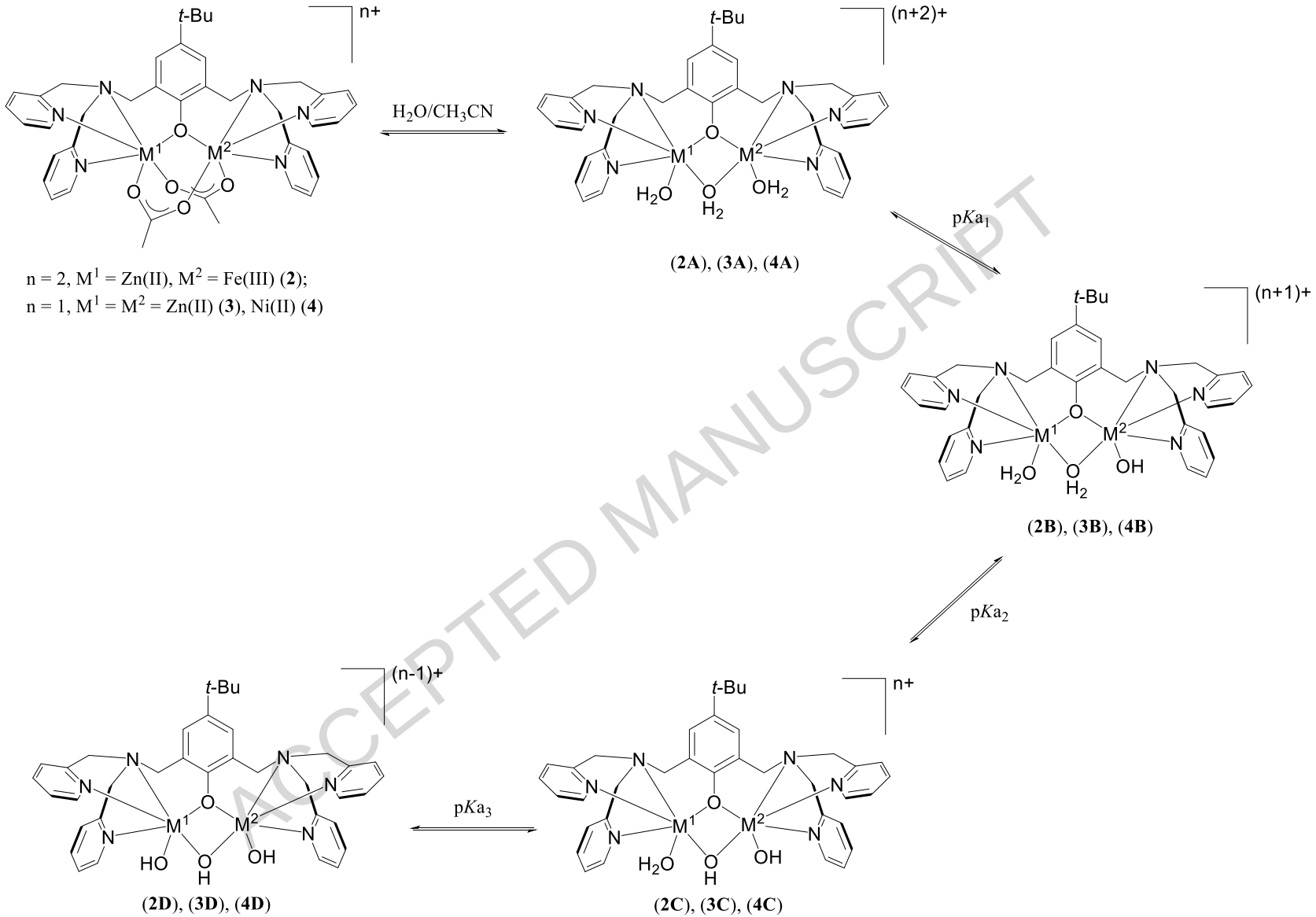
[Ni(II)−Ni(II)] (**4**) complexes came from the observation of isobestic points at different pH ranges for these complexes. Specifically, the heterodinuclear [Zn(II)−Fe(III)] (**2**) complex displayed three isobestic points at the pH range of 5.65–6.00, 6.15–6.50 and 6.65–7.10. The homodinuclear [Zn(II)−Zn(II)] (**3**) complex, too showed three isobestic points at the pH range of 6.8–9.2. The homodinuclear [Ni(II)−Ni(II)] (**3**) complex, exhibited two isobestic points at the pH range of 6.8–9.6 and 9.6–13.2. These isobestic points represented the interconversion between the triaquated species, $\{L[(H_2O)Zn^{II}(\mu\text{–}H_2O)Fe^{III}(H_2O)]\}^{4+}$ (**2A**), $\{L[(H_2O)Zn^{II}(\mu\text{–}H_2O)Zn^{II}(H_2O)]\}^{3+}$ (**3A**) and $\{L[(H_2O)Ni^{II}(\mu\text{–}H_2O)Ni^{II}(H_2O)]\}^{3+}$ (**4A**), to the diaquated and monohydroxo species, $\{L[(H_2O)Zn^{II}(\mu\text{–}H_2O)Fe^{III}(OH)]\}^{3+}$ (**2B**), $\{L[(H_2O)Zn^{II}(\mu\text{–}H_2O)Zn^{II}(OH)]\}^{2+}$ (**3B**) and $\{L[(H_2O)Ni^{II}(\mu\text{–}H_2O)Ni^{II}(OH)]\}^{2+}$ (**4B**), to the monoaquated and dihydroxospecies, $\{L[(H_2O)Zn^{II}(\mu\text{–}OH)Fe^{III}(OH)]\}^{2+}$ (**2C**), $\{L[(H_2O)Zn^{II}(\mu\text{–}OH)Zn^{II}(OH)]\}^{+}$ (**3C**) and $\{L[(H_2O)Ni^{II}(\mu\text{–}OH)Ni^{II}(OH)]\}^{+}$ (**4C**)]), to the trihydroxo species, $\{L[(HO)Zn^{II}(\mu\text{–}OH)Fe^{III}(OH)]\}^{+}$ (**2D**), $\{L[(OH)Zn^{II}(\mu\text{–}OH)Zn^{II}(OH)]\}$ (**3D**) and $\{L[(H_2O)Ni^{II}(\mu\text{–}OH)Ni^{II}(OH)]\}$ (**4D**)] (Scheme 2). These isobestic points corresponded to the pK_a values of 5.76 (pK_{a1}), 6.29 (pK_{a2}) and 6.97 (pK_{a3}) for the heterodinuclear [Zn(II)−Fe(III)] (**2**) complex, a pK_a value in the range of 7.11–7.87 in case of the homodinuclear [Zn(II)−Zn(II)] (**3**) complex and the pK_a values of 7.69 (pK_{a1}), and 10.81 (pK_{a2}) in case of the homodinuclear [Ni(II)−Ni(II)] (**4**) complex. Significantly enough, the monoaquated and dihydroxo species of the intermediates, $\{L[(H_2O)Zn^{II}(\mu\text{–}OH)Fe^{III}(OH)]\}^{2+}$ (**2C**) and $\{L[(H_2O)Zn^{II}(\mu\text{–}OH)Zn^{II}(OH)]\}^{+}$ (**3C**), and the trihydroxo species, $\{L[(HO)Zn^{II}(\mu\text{–}OH)Fe^{III}(OH)]\}^{+}$ (**2D**), $\{L[(HO)Zn^{II}(\mu\text{–}OH)Zn^{II}(OH)]\}$ (**3D**) and $\{L[(HO)Ni^{II}(\mu\text{–}OH)Ni^{II}(OH)]\}$ (**4D**) have been detected by ESI-MS studies (Supporting Information Figures S11, S12, S31, S32, S49). More importantly, based on the reports of a

ACCEPTED MANUSCRIPT

monoaquated and dihydroxo species being the active species of the PAP [96] and zinc phosphoesterase [17] enzymes, the analogues $\{L[(H_2O)Zn^{II}(\mu\text{–}OH)Fe^{III}(OH)]\}^{2+}$ (**2C**), $\{L[(H_2O)Zn^{II}(\mu\text{–}OH)Zn^{II}(OH)]\}^{+}$ (**3C**) and $\{L[(H_2O)Ni^{II}(\mu\text{–}OH)Ni^{II}(OH)]\}^{+}$ (**4C**), are assigned as the active species for the phosphoester cleavage reaction at the pH range of 6.15–9.60 with the pK_a values of 6.29, 7.11−7.87 and 7.69 respectively.

The zinc center of the monoaquated and dihydroxo species $\{L[(H_2O)Zn^{II}(\mu\text{–}OH)Fe^{III}(OH)]\}^{2+}$, (**2C**) and $\{L[(H_2O)Zn^{II}(\mu\text{–}OH)Zn^{II}(OH)]\}^{+}$ (**3C**), and the nickel center of the monoaquated and dihydroxo species $\{L[(H_2O)Ni^{II}(\mu\text{–}OH)Ni^{II}(OH)]\}^{+}$ (**4C**) contains a metal bound labile H_2O molecule [Zn(II)−(H_2O)] (**2C** and **3C**), and [Ni(II)−(H_2O)] (**4C**) which makes way to the incoming substrate *bis*(2,4−dinitrophenyl)phosphate (2,4−BDNPP). The other metal center *i.e.* the Fe(III) center in the $\{L[(H_2O)Zn^{II}(\mu\text{–}OH)Fe^{III}(OH)]\}^{2+}$ (**2C**) species, the Zn(II) center in the $\{L[(H_2O)Zn^{II}(\mu\text{–}OH)Zn^{II}(OH)]\}^{+}$ (**3C**) species, and the Ni(II) center in the $\{L[(H_2O)Ni^{II}(\mu\text{–}OH)Ni^{II}(OH)]\}^{+}$ (**4C**) species, contain a metal bound terminal hydroxo moiety namely, [Fe(III)−(OH)] in **2C**, [Zn(II)−(OH)] in **3C** and [Ni(II)−(OH)] in **4C** which participate in a nucleophilic attack on the P atom of the metal bound 2,4−BDNPP substrate resulting in the phosphoester cleavage.

ACCEPTED MANUSCRIPT



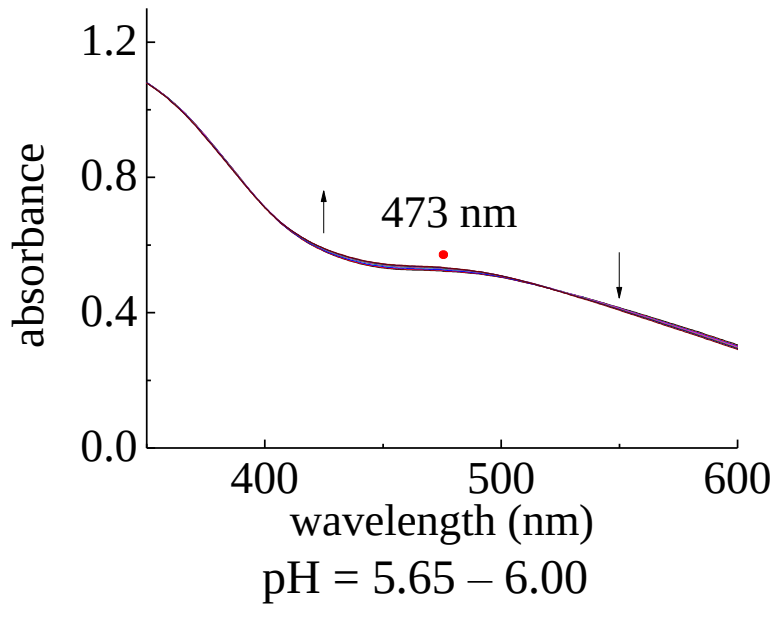
Scheme 2. Equilibrium of chemical species in CH_3CN/H_2O solution proposed for the hetero- and homodinuclear complexes (**2**–**4**) supported over symmetrical ligand **1**.

ACCEPTED MANUSCRIPT

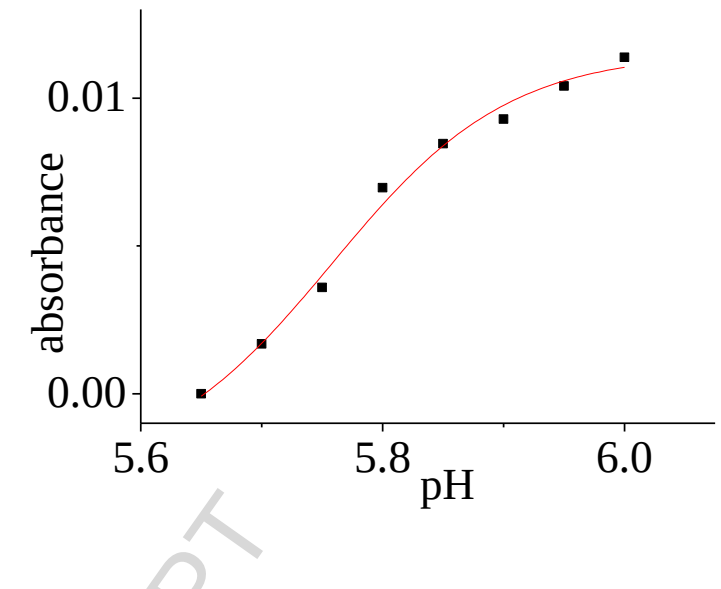
Figure 3. Electronic spectrum (Column 1) in different pH ranges [(*a*) 5.65 – 6.00, (*b*) 6.15 – 6.50, (*c*) 6.65 – 7.10] and the corresponding titration plot (Column 2) performed at 473 nm (LMCT band) as a function of pH with incremental additions of 0.1 M NaOH [5 μL] in an CH_3CN/H_2O (*v/v* 1:1) solution of **2** (6.0×10^{-4} M) containing I = 0.1 M (KCl).

S.No.	electronic spectrum	Sigmoidal curve fit

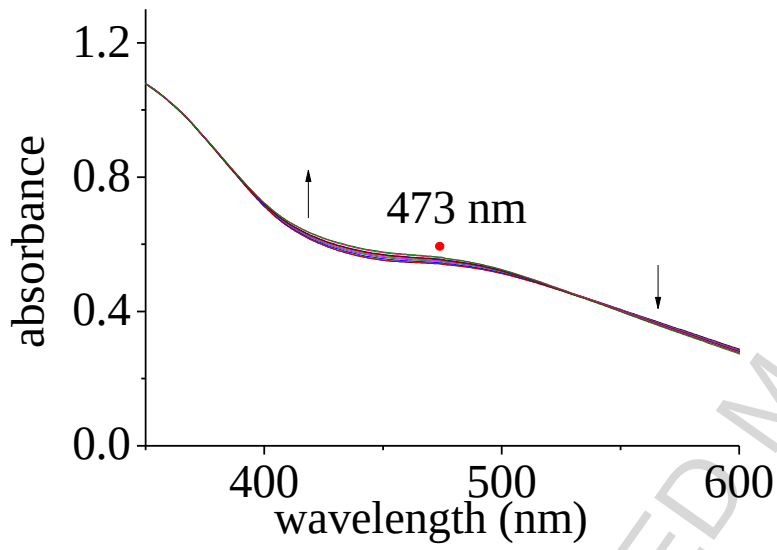
(a)



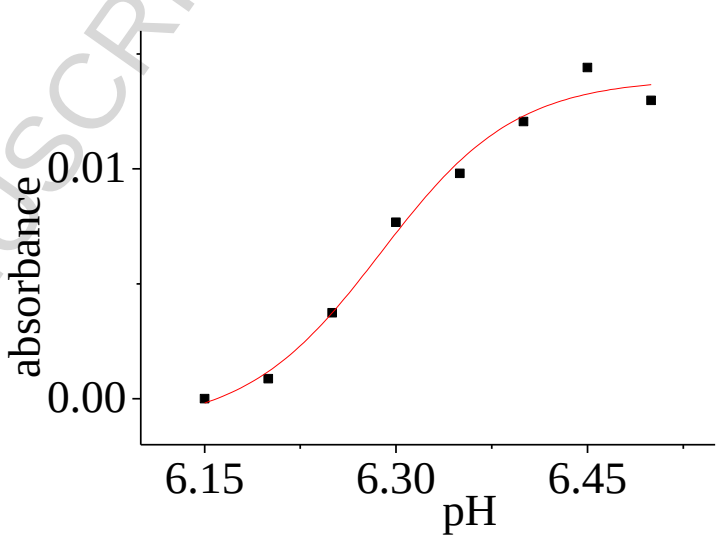
pH = 5.65 – 6.00



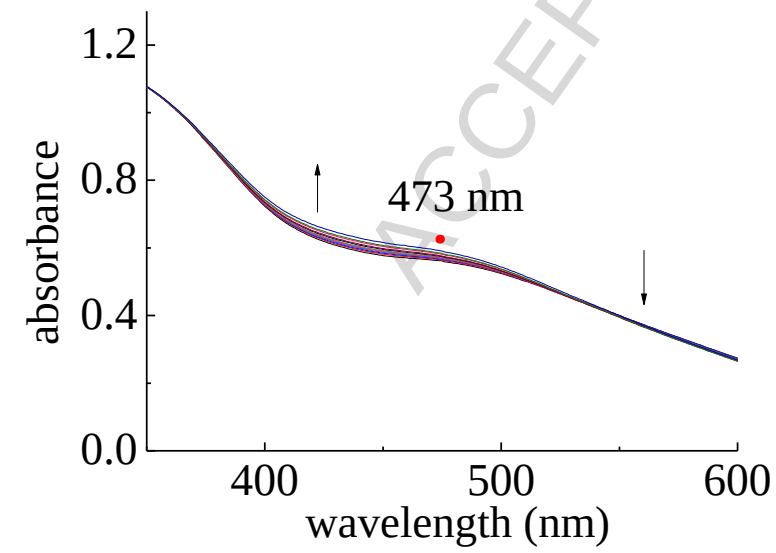
(b)



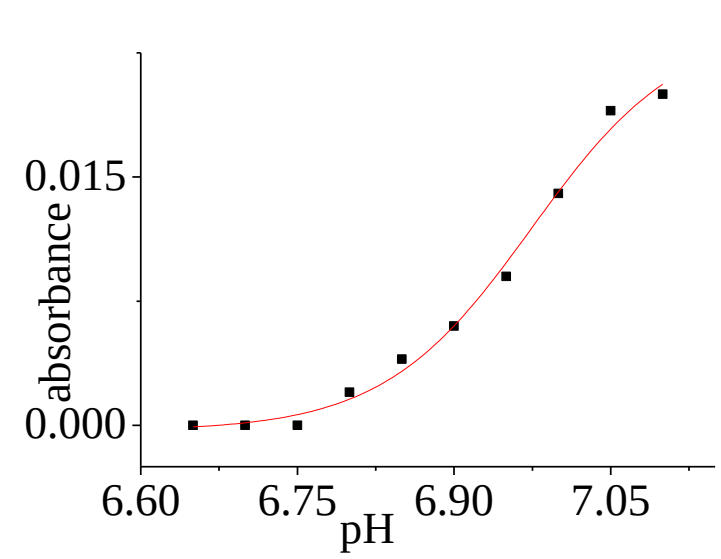
pH = 6.15 – 6.50



(c)



pH = 6.65 – 7.10



ACCEPTED MANUSCRIPT

Table 5. Spectrophotometric titration data of **2**, **3** and **4**.

S. No.	Metal complex	λ_{max}(nm)	pKa	
1.	**2** [Zn(II)–Fe(III)]	473	pKa_1	5.76
			pKa_2	6.29
			pKa_3	6.97
2.	**3** [Zn(II)–Zn(II)]	220	pKa	7.87
		259	pKa	7.11
		295	pKa	7.53
3.	**4** [Ni(II)–Ni(II)]	303	pKa_1	7.69
			pKa_2	10.81

ACCEPTED MANUSCRIPT

Quite importantly, the hydrolysis of *bis*(2,4−dinitrophenyl)phosphate (2,4−BDNPP) was successfully performed by the heterodinuclear [Zn(II)–Fe(III)] (**2**) complex and the homodinuclear [Zn(II)−Zn(II)] (**3**) and [Ni(II)−Ni(II)] (**4**)] complexes in a mixed medium of CH_3CN/H_2O (*v/v* 1:1) in the pH range of 5.5−10.5 at room temperature, by monitoring spectrophotometrically the reaction at 400 nm (ε = 12100 $M^{-1}cm^{-1}$) corresponding to a band from the 2,4-DNP^- anion at 25 ℃, as reported in literature [69].

A bell shaped pH profile was observed in the pH range of 5.5−9.0 with a rate maxima at pH 6.5 for the heterodinuclear [Zn(II)–Fe(III)] (**2**) complex (Figure 4) analogous to that of the related [Zn(II)−Fe(III)] complexes which also showed a rate maxima at pH 6.5 [69, 94] and also to that of the PAP enzyme that showed a rate maxima at pH 4.9 [114]. Sigmoidal fit to the decline part of the pH profile curve gave a pK_a value of 8.28 closer to the pK_{a3} value of 6.97 as obtained from the spectrophotometric titration studies. The difference in the pK_a values between the two data can be explained on the fact that the spectrophotometric titration pK_a value is obtained for the free catalyst while the kinetic pK_a value from the initial rate (V_0) *versus* pH plot is due to the catalyst–substrate complex [65]. The homodinuclear [Zn(II)−Zn(II)] (**3**) complex however, showed highest activity at pH 8 with a bell shaped pH profile (Figure 4). Bell shaped fit to the pH range of 5.5−9.0 of the initial rate (V_0) *versus* pH plot gave a pK_a value of 6.99 in concurrence to the pK_a values *ca*. 7.11−7.87 obtained from the spectrophotometric titration studies. Quite interestingly, the homodinuclear [Ni(II)−Ni(II)] (**3**) complex showed a sigmoidal pH profile (Figure 4) with the highest activity at pH 10.5. Sigmoidal fit of the initial rate (V_0) *versus* pH plot gave a pK_a value of 8.05 in concurrence to the pK_{a2} value 10.81 obtained from the spectrophotometric titration studies.

ACCEPTED MANUSCRIPT

The pK_a values obtained from the sigmoidal fit of the pH profile curves give valuable insights about the nature and the concentration of the active species present in equilibrium in solution as a function of pH. In particular, for the heterodinuclear [Zn(II)−Fe(III)] (**2**) complex, the maximum initial rate (V_0) observed at the pH ranges that fall between pK_{a1} and pK_{a2} values obtained from spectrophotometric titration studies, indicated the monoaquated and dihydroxo species of the type $\{L[(H_2O)Zn^{II}(\mu\text{–}OH)Fe^{III}(OH)]\}^{2+}$ (**2C**), to be the active species in the phosphoester hydrolysis reaction, in concurrence with that of purple acid phosphatases (PAPs) [114, 115] and the related Zn(II)−Fe(III) complexes [66, 69, 94, 116]. Similarly, for the homodinuclear Zn(II)−Zn(II)] (**3**) and [Ni(II)−Ni(II)] (**4**) complexes, the alignment of the pK_a values obtained from both kinetic studies and spectrophotometric titration studies showed that the monoaquated and dihydroxo species of the type $\{L[(H_2O)M^1(\mu\text{–}OH)M^2(OH)]\}^+$ [$M^1 = M^2$ = Zn (**3C**), Ni (**4C**)] to be the active species in the phosphoester hydrolysis reaction.

Under limiting conditions the reaction rate for the phosphoester hydrolysis decreases as a result of decrease in the concentration of the monoaquated and dihydroxo species, $\{L[(H_2O)Zn^{II}(\mu\text{–}OH)Fe^{III}(OH)]\}^{2+}$ (**2C**), $\{L[(H_2O)Zn^{II}(\mu\text{–}OH)Zn^{II}(OH)]\}^+$ (**3C**), and $\{L[(H_2O)Ni^{II}(\mu\text{–}OH)Ni^{II}(OH)]\}^+$ (**4C**)]. For example, at a lower pH predominance of the triaquated species $\{L[(H_2O)Zn^{II}(\mu\text{–}H_2O)Fe^{III}(H_2O)]\}^{4+}$ (**2A**), $\{L[(H_2O)Zn^{II}(\mu\text{–}H_2O)Zn^{II}(H_2O)]\}^{3+}$ (**3A**) and $\{L[(H_2O)Ni^{II}(\mu\text{–}H_2O)Ni^{II}(H_2O)]\}^{3+}$ (**4A**) occur leading to a slower reaction rate of phosphoester hydrolysis as catalyzed by the lower concentration of the monoaquated and dihydroxo species, $\{L[(H_2O)Zn^{II}(\mu\text{–}OH)Fe^{III}(OH)]\}^{2+}$ (**2C**), $\{L[(H_2O)Zn^{II}(\mu\text{–}OH)Zn^{II}(OH)]\}^+$ (**3C**), and $\{L[(H_2O)Ni^{II}(\mu\text{–}OH)Ni^{II}(OH)]\}^+$ (**4C**). Similarly, at extremely high pH, the trihydroxo species

ACCEPTED MANUSCRIPT

$\{L[(HO)Zn^{II}(\mu\text{–}OH)Fe^{III}(OH)]\}^{+}$ (**2D**) and $\{L[(HO)M^{1}(\mu\text{–}OH)M^{2}(OH)]\}$ [$M^1 = M^2$ = Zn (**3D**), Ni (**4D**)] is predominant leading to a decrease in the reaction rate arising from a lower concentration of the monoaquated and dihydroxo species, $\{\{L[(H_2O)Zn^{II}(\mu\text{–}OH)Fe^{III}(OH)]\}^{2+}$ (**2C**), $\{L[(H_2O)\ M^{1}(\mu\text{–}OH)\ M^{2}(OH)]\}^{+}$ [$M^1 = M^2$ = Zn (**3C**), Ni (**4C**)].

Saturation kinetics was performed at pH 6.5 for both of the heterodinuclear [Zn(II)–Fe(III)] (**2**) and the homodinuclear [Zn(II)–Zn(II)] (**3**) complexes and at pH 8.0 for the homodinuclear [Ni(II)–Ni(II)] (**4**) complex with respect to the substrate concentration and the data so obtained was fitted to the Michaelis-Menten equation. Linearization of the curves using the Lineweaver-Burk method gave the K_m, V_{max} and k_{cat} parameter (Table 6).

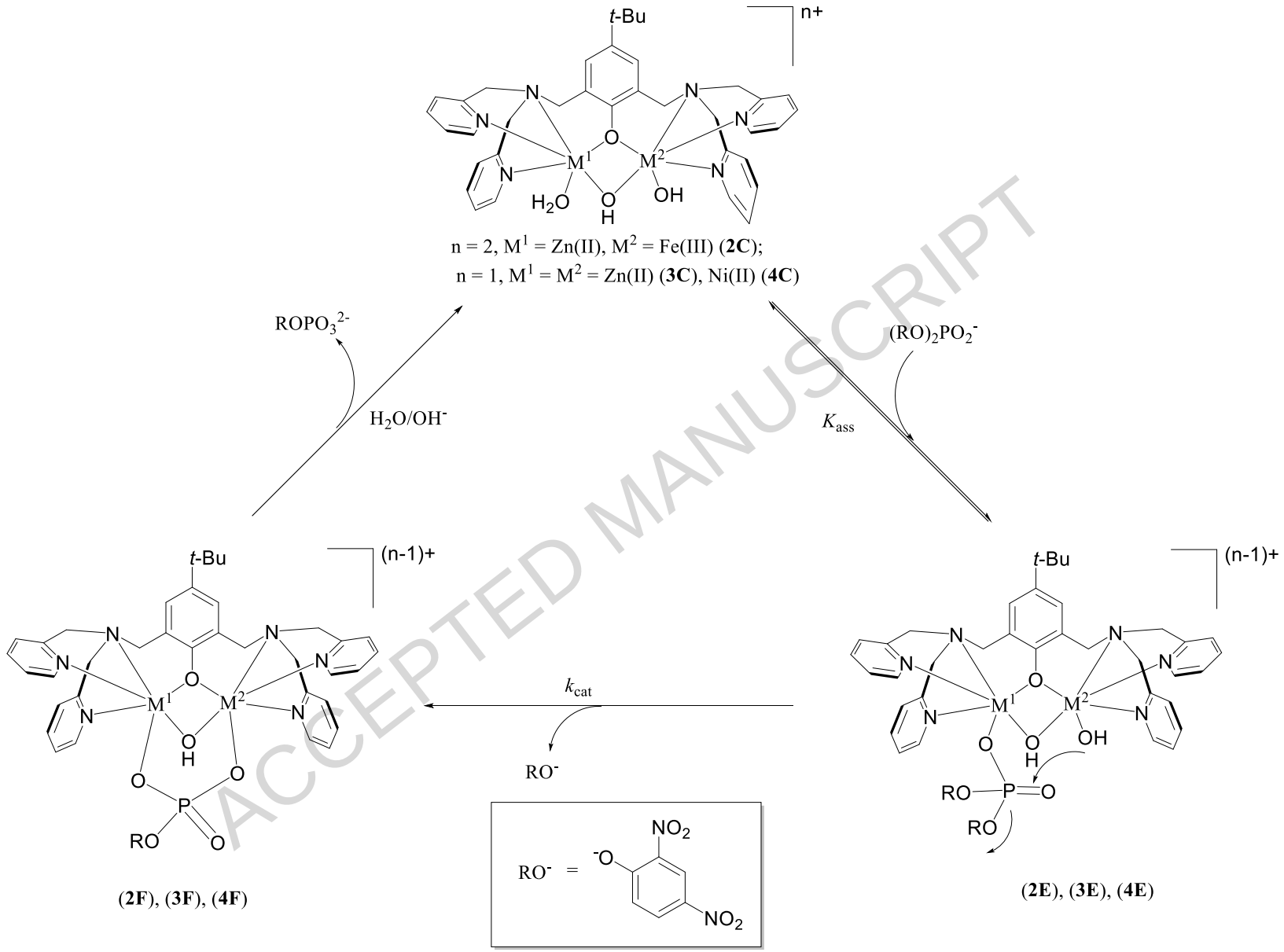
It is quite interesting to note that the heterodinuclear [Zn(II)–Fe(III)] (**2**) complex displayed a weak affinity towards the substrate (2,4−BDNPP) as evident from its higher K_m value of 1.64 ± 0.37 mM and lower K_{ass} ($K_{ass} \cong 1/K_m$) value of 0.61 mM^{-1} as compared to the homodinuclear [Zn(II)–Zn(II)] (**3**) and [Ni(II)–Ni(II)] (**4**) complexes, which showed stronger affinity towards the substrate (2,4−BDNPP) as evident from their lower K_m value of 1.23 ± 0.29 mM (**3**) and 0.286 ± 0.02 mM (**4**) and higher K_{ass} value of 0.81 mM^{-1} (**3**) and 3.49 mM^{-1} (**4**). The k_{cat} value for the heterodinuclear [Zn(II)–Fe(III)] (**2**) complex (*ca.* 4.62×10^{-4} s^{-1}) was found to be significantly lower than the similar [Zn(II)–Fe(III)] complexes known in the literature [6.76×10^{-4} s^{-1} – 9.13×10^{-4} s^{-1}] [66, 69, 76] but comparable to an unsymmetrical [Zn(II)–Fe(III)] counterpart (0.40×10^{-4} s^{-1}) [94]. The homodinuclear [Zn(II)–Zn(II)] (**3**) complex with the k_{cat} value of *ca.* 3.23×10^{-4} s^{-1} also exhibited lower activity towards the phosphoester hydrolysis as compared to the related homodinuclear [Zn(II)–Zn(II)] complexes known in the literature [6.40 ×

ACCEPTED MANUSCRIPT

10^{-4} s^{-1} – 5.70 × 10^{-3} s^{-1}] [59, 75, 77, 81]. Quite interestingly, the homodinuclear [Ni(II)–Ni(II)] (**4**) complex with the k_{cat} value of *ca.* 1.26 × 10^{-2} s^{-1} also exhibited higher activity towards the phosphoester hydrolysis as compared to the related homodinuclear [Ni(II)–Ni(II)] complexes known in the literature [2.80 × 10^{-3} s^{-1}] [100]. Significantly enough, the rate of the hydrolysis of the 2,4−BDNPP substrate as catalyzed by the heterodinuclear [Zn(II)–Fe(III)] (**2**) complex and the homodinuclear [Zn(II)–Zn(II)] (**3**) and [Ni(II)–Ni(II)] (**4**) complexes are *ca.* 10100−394000 times faster than the uncatalysed reaction under the similar conditions [117].

ACCEPTED MANUSCRIPT

ACCEPTED MANUSCRIPT



Scheme 3. Proposed mechanism for the hydrolysis of 2,4-*bis*(dinitrophenyl)phosphate as catalyzed by a the hetero- and homodinuclear complexes (**2**–**4**) supported over symmetrical ligand **1**..

ACCEPTED MANUSCRIPT

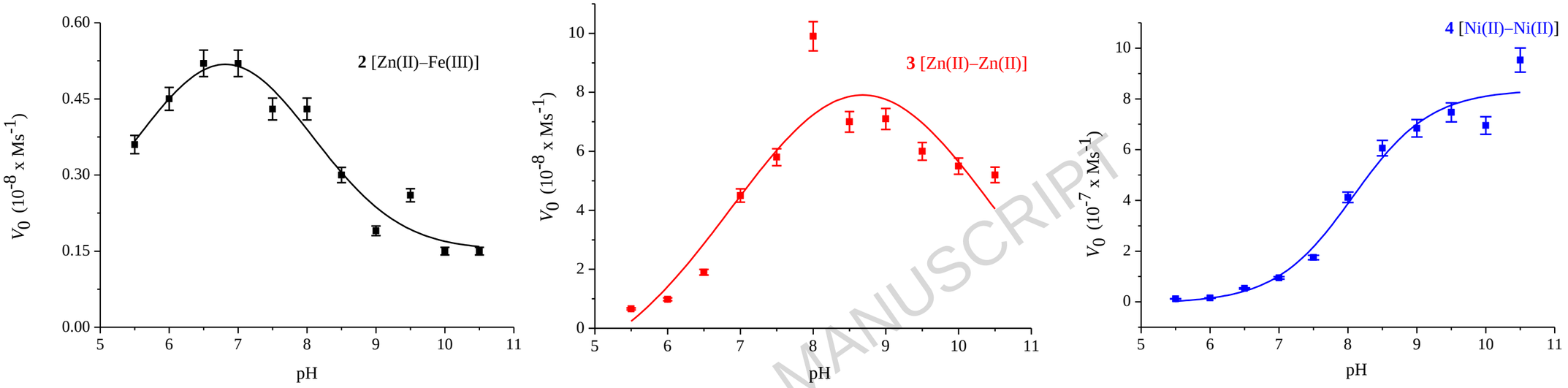


Figure 4. The pH profiles of the initial rates for the hydrolysis of *bis*(2,4−dinitrophenyl)phosphate (2,4−BDNPP) as catalyzed by {L[Zn^{II}(μ–OAc)$_2$$Fe^{III}$]}($BPh_4$)$_2$ (**2**) (**A**), {L[Zn^{II}(μ–OAc)$_2$$Zn^{II}$]}$BPh_4$ (**3**) (**B**) and {L[Ni^{II}(μ–OAc)$_2$$Ni^{II}$]}$BPh_4$ (**4**) (**C**) type complexes in CH_3CN/H_2O (*v/v* 1:1).

ACCEPTED MANUSCRIPT

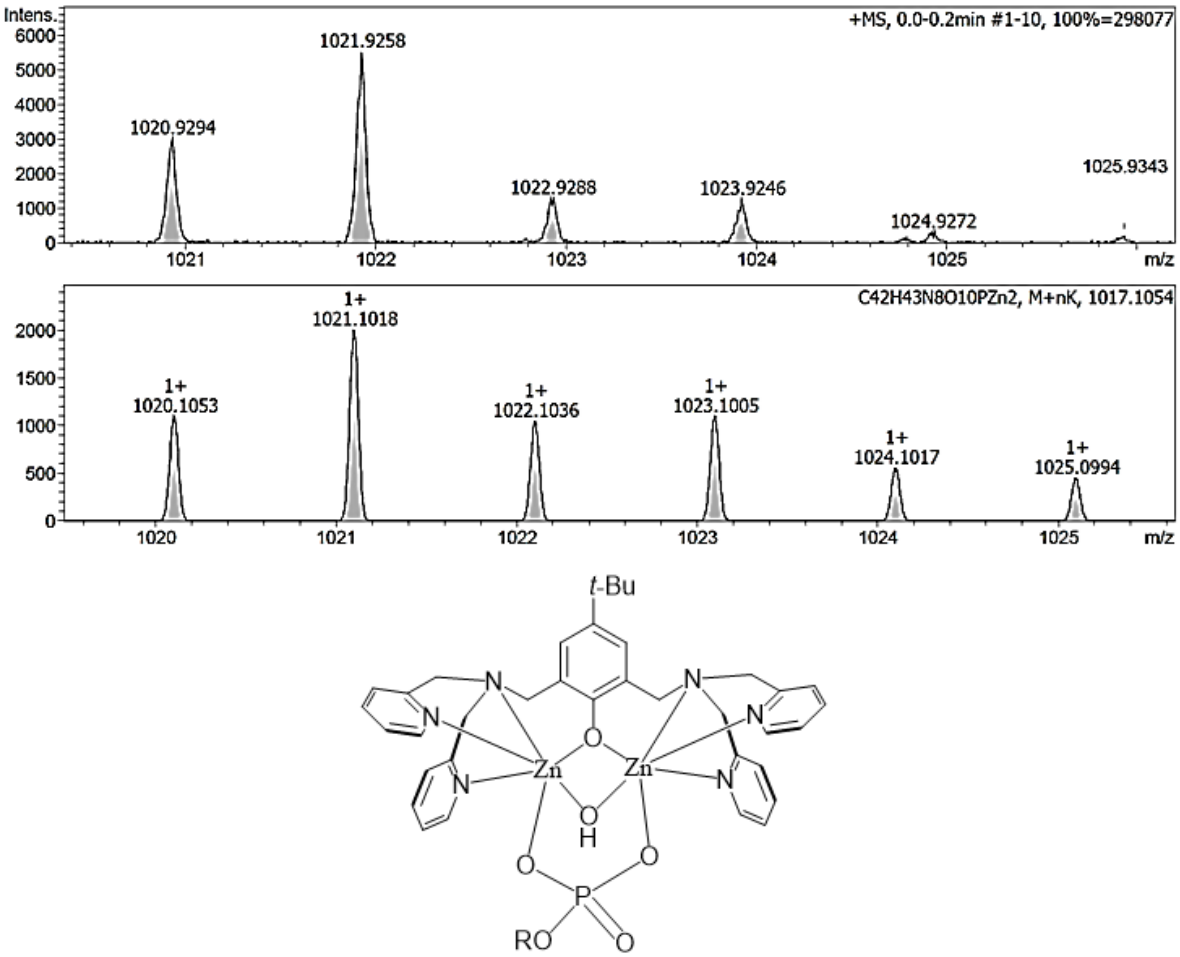
Table 6. Kinetic parameters of complexes **2**, **3** and **4**.

S.No.	Complex	K_M (mM)	K_{ass} (mM^{-1})	V_{max} ($10^{-8} \times Ms^{-1}$)	k_{cat} (s^{-1})	k_{cat}/K_M ($M^{-1}s^{-1}$)	k_{cat}/k_{uncat} (10^4)
1.	**2** [Zn(II)–Fe(III)]	1.64 ± 0.37	0.609	2.28	4.62×10^{-4}	2.82×10^{-4}	1.44
2.	**3** [Zn(II)–Zn(II)]	1.23 ± 0.29	0.813	1.60	3.24×10^{-4}	2.60×10^{-4}	1.01
3.	**4** [Ni(II)–Ni(II)]	0.286 ± 0.02	3.49	62.8	1.26×10^{-2}	4.40×10^{-2}	39.4

Reaction condition: 0.05 mM catalyst (**2**/**3**/**4**), 0.5-4.0 mM *bis*(2,4-dinitrophenyl)phosphate and 0.05 M buffer [pH = 6.5 (**2**/**3**) and 8.0 (**4**)] with ionic strength of 0.1 M $NaClO_4$ in a total 2.5 mL CH_3CN:H_2O (*v/v* 1:1) at 25 ºC. $k_{uncat} = 3.2 \times 10^{-8}$ s^{-1} [117].

ACCEPTED MANUSCRIPT

ACCEPTED MANUSCRIPT



(3F)

Figure 5. The catalytically active intermediate specie, {L[Zn^{II}(μ–OH)(μ–RPO_4)Zn^{II}]} (**3F**) of a representative homodinuclear complex (**3**) that has been detected in mass spectrometry studies.

ACCEPTED MANUSCRIPT

Mechanistic discussion and its detection by mass spectrometry

Based on the UV-vis experiments and saturated kinetics studies a plausible mechanism has been proposed for the hydrolysis of 2,4−BDNPP substrate by the heterodinuclear [Zn(II)−Fe(III)] (**2**) and the homodinuclear [Zn(II)−Zn(II)] (**3**) and [Ni(II)−Ni(II)] (**4**)] complexes (Scheme 3). At the pH range 6.15–7.15, the active species in the form of monoaquated and dihydroxo $\{L[(H_2O)Zn^{II}(\mu\text{–}OH)Fe^{III}(OH)]\}^{2+}$ (**2C**), $\{L[(H_2O)Zn^{II}(\mu\text{–}OH)Zn^{II}(OH)]\}^{+}$ (**3C**) and $\{L[(H_2O)M^{II}(\mu\text{–}OH)M^{II}(OH)]\}^{+}$ (**4C**) type intermediates reacts with the 2,4−BDNPP substrate replacing the metal bound water moiety [M(II)–H_2O] and giving rise to the corresponding metal bound substrate species of the type $\{L[(R_2PO_4)Zn^{II}(\mu\text{–}OH)Fe^{III}(OH)]\}^{+}$ (**2E**) $\{L[(R_2PO_4)Zn^{II}(\mu\text{–}OH)Zn^{II}(OH)]\}$ (**3E**) and $\{L[(R_2PO_4)Ni^{II}(\mu\text{–}OH)Ni^{II}(OH)]\}$ (**4E**). Significantly enough, the former species, $\{L[(R_2PO_4)Zn^{II}(\mu\text{–}OH)Fe^{III}(OH)]\}^{+}$ (**2E**), has been detected by mass spectrometry (Supporting Information Figure. S21).

Subsequent intramolecular nucleophilic attack by the metal bound hydroxo moiety Fe(III)−(OH) in $\{L[(R_2PO_4)Zn^{II}(\mu\text{–}OH)Fe^{III}(OH)]\}^{+}$ (**2E**), and M(II)−(OH) moiety in $\{L[(R_2PO_4)M^{II}(\mu\text{–}OH)M^{II}(OH)]\}$ [M = Zn (**3E**), Ni (**4E**)], on to the P atom of the metal bound substrate 2,4−BDNPP leads to the formation of $\{L[Zn^{II}(\mu\text{–}OH)(\mu\text{–}RPO_4)Fe^{III}]\}^{+}$ (**2F**), $\{L[Zn^{II}(\mu\text{–}OH)(\mu\text{–}RPO_4)Zn^{II}]\}$ (**3F**) and $\{L[Ni^{II}(\mu\text{–}OH)(\mu\text{–}RPO_4)Ni^{II}]\}$ (**4F**), type intermediates with the subsequent release of the phosphodiester cleavage product, 2,4–dinitrophenolate (2,4–DNP) in the process. The intermediates $\{L[Zn^{II}(\mu\text{–}OH)(\mu\text{–}RPO_4)Fe^{III}]\}^{+}$ (**2F**), and $\{L[Zn^{II}(\mu\text{–}OH)(\mu\text{–}RPO_4)Zn^{II}]\}$ (**3F**), have been detected using mass spectrometry study (Figure 5 and Supporting Information Figure. S23).

ACCEPTED MANUSCRIPT

The intermediates $\{L[Zn^{II}(\mu\text{–}OH)(\mu\text{–}RPO_4)Fe^{III}]\}^+$ (**2F**), $\{L[Zn^{II}(\mu\text{–}OH)(\mu\text{–}RPO_4)Zn^{II}]\}$ (**3F**), and $\{L[Ni^{II}(\mu\text{–}OH)(\mu\text{–}RPO_4)Ni^{II}]\}$ (**4F**), reacts further with H_2O giving the hydrolyzed product 2,4-dinitrophenyl phosphate (2,4–DNPP) along with the monoaquated and dihydroxo $\{L[(H_2O)Zn^{II}(\mu\text{–}OH)Fe^{III}(OH)]\}^{2+}$ (**2C**), and $\{L[(H_2O)Zn^{II}(\mu\text{–}OH)Zn^{II}(OH)]\}^+$ (**3C**) and $\{L[(H_2O)Ni^{II}(\mu\text{–}OH)Ni^{II}(OH)]\}^+$ (**4C**).

Conclusion

In summary, the heterodinuclear mixed valence [Zn(II)−Fe(III)] (**2**) complex and the homodinuclear [Zn(II)−Zn(II)] (**3**) and [Ni(II)−Ni(II)] (**4**) complexes successfully carried out the hydrolysis of 2,4-BDNPP substrate similar to that of the PAP and zinc phosphoesterase enzymes. Between the three, the heterodinuclear [Zn(II)−Fe(III)] (**2**) complex showed higher K_m value of 1.64 ± 0.37 mM and lower K_{ass} value of 0.61 mM^{-1} as compared to the homodinuclear [Zn(II)−Zn(II)] (**3**) complex [K_m = 1.23 ± 0.29 mM and K_{ass} = 0.81 mM^{-1}] and [Ni(II)−Ni(II)] (**3**) complex [K_m = 0.286 ± 0.02 mM and K_{ass} = 3.51 mM^{-1}] signifying a strong affinity of the homodinuclear [Ni(II)−Ni(II)] (**4**) complex towards the substrate (2,4−BDNPP). The homodinuclear [Ni(II)−Ni(II)] (**3**) complex ($k_{cat} = 1.26 \times 10^{-2}$) showed higher activity towards the phosphoester hydrolysis as compared to the homodinuclear [Zn(II)−Zn(II)] (**3**) complex ($k_{cat} = 3.24 \times 10^{-4}$ s^{-1}) and the heterodinuclear [Zn(II)−Fe(III)] (**2**) complex ($k_{cat} = 4.62 \times 10^{-4}$ s^{-1}). It is important to note that, given the differences that exist between the model complexes to that of the real enzymes, in which the active-site pockets exercise significant influences on the enzyme catalyse, a direct comparison of the rate constants of our model complexes (**2**–**4**) to that of real enzymes becomes challenging. The monoaquated and dihydroxo species, $\{L[(H_2O)Zn^{II}(\mu\text{–}OH)Fe^{III}(OH)]\}^{2+}$ (**2C**) and $\{L[(H_2O)Zn^{II}(\mu\text{–}OH)Zn^{II}(OH)]\}^+$ (**3C**), and the trihydroxo species, $\{L[(HO)Zn^{II}(\mu\text{–}OH)Fe^{III}(OH)]\}^+$ (**2D**), $\{L[(HO)Zn^{II}(\mu\text{–}OH)Zn^{II}(OH)]\}$ (**3D**) and $\{L[(HO)Ni^{II}(\mu\text{–}$

ACCEPTED MANUSCRIPT

OH)Ni^{II}(OH)]} (**4D**), as generated in the CH_3CN/H_2O (*v/v* 1:1) mixed medium have been detected by mass spectrometry. In addition, the catalyst–substrate adduct species of the type {L[Zn^{II}(μ–OH)(μ–RPO_4)Fe^{III}]}$^+$ (**2F**), and {L[Zn^{II}(μ–OH)(μ–RPO_4)Zn^{II}]} (**3F**), have also been detected by mass spectrometry.

ACCEPTED MANUSCRIPT

ACCEPTED MANUSCRIPT

Experimental section

General Procedures. All manipulations were carried out using a combination of a glovebox and standard Schlenk techniques. 2-aminomethylpyridine was obtained from AldrichChemical Co., while all the other chemicals used are from spectrochem (India) were used without any further purification. 2,6-*bis*(hydroxymethyl)-4-*t*-butylphenol [118], 2,6-*bis*(chloromethyl)-4-*t*-butylphenol [111], *bis*(2-pyridylmethyl)amine [56], 2,6-*bis*{[*bis*(2-pyridylmethyl)amino]methyl}-4-*t*-butylphenol [45] and 2,4-*bis*-dinitrophenyl phosphate [117] were synthesized according to modified literature procedures. ^{1}H NMR and ^{13}C{^{1}H} NMR spectra were recorded on a Bruker 400 MHz and Bruker 500 MHz NMR spectrometer. ^{1}H NMR peaks are labeled as singlet (s), doublet (d), triplet (t), quartet (q), quartet of doublets (qd), doublet of doublets (dd), septet (sept) and broad (br). The electronic spectra of **2** and **3** complexes are recorded in CH_3CN using a UV 3600 Shimadzu and Cary Bio spectrophotometer. Mass spectrometry measurements were done on a Micromass Q-Tof spectrometer and Bruker maxis impact spectrometer. Elemental Analysis was carried out on Thermo Finnigan FLASH EA 1112 SERIES (CHNS) Elemental Analyzer. The variable temperature magnetic experiments were executed in SQUID-VSM, quantum design, USA and the data was fitted using PHI software [112].

X-ray crystallography

X-ray diffraction data for compounds **2**, **3** and **4** were collected on an APEXII, Bruker-AXS and Rigaku Hg 724+ diffractometer respectively, for unit cell determination and intensity data collection. Data integration and indexing were carried out using Rigaku suite of programs CrystalClear and CrystalStructure. Structure refinement and geometrical calculations were carried out using programs in the WinGX module [119]. The final structure refinement was carried out using full least squares methods on F^2 using SHELXL-

ACCEPTED MANUSCRIPT

2014 [120]. Crystal data collection and refinement parameters are summarized in Supporting Information Table S1. CCDC-926964 (for **2**), CCDC-928807 (for **3**) and CCDC-1585928 (for **4**) contain the supplementary crystallographic data for this chapter. These data can be obtained free of charge from the Cambridge Crystallographic Data center *via* www.ccdc.cam.ac.uk/data_request/cif.

Synthesis of {L[$Zn^{II}(\mu$–OAc)$_2Fe^{III}$]}$(BPh_4)_2$ (2)

A solution of 2,6-*bis*{[*bis*(2-pyridylmethyl)amino]methyl}-4-*t*-butylphenol (**1**) (0.250 g, 0.436 mmol) in MeOH (15.0 mL) was treated with a solution of $Fe(NO_3)_3$•$9H_2O$ (0.176 g, 0.436 mmol) in MeOH (5.00 mL) resulting in a dark-blue solution, to which a solution of $Zn(OAc)_2$•$2H_2O$ (0.095 g, 0.434 mmol) in MeOH (*ca.* 5 mL) was subsequently added followed by the addition of a solution of NaOAc•$3H_2O$ (0.237 g, 1.74 mmol) in MeOH (5.00 mL). The resulting solution was stirred for 10 minutes at room temperature. A solution of $NaBPh_4$ (0.596 g, 1.74 mmol) in MeOH (5.00 mL) was added to the reaction mixture resulting in a precipitate, which was filtered and dried under vacuum to obtain crude product. The crude product was further purified by vapour diffusion of MeOH into an acetone solution of crude product to get the product after 4 days as a dark blue crystalline solid (**2**) (0.238 g, 37 %). IR data (KBr pellet) cm^{-1}: 3437 (w), 3054 (w), 3035 (w), 1606 (s), 1580 (w), 1480 (m), 1427 (m), 1332 (w), 1306 (w), 1290 (w), 1265 (w), 1217 (w), 1157 (w), 1097 (w), 1052 (w), 1023 (w), 941 (w), 878 (w), 832 (w), 763 (w), 733 (m), 704 (m), 650 (w), 612 (w), 577 (w), 529 (w). HRMS (ES): *m/z* 404.6039 $[M–2BPh_4]^{2+}$, Calcd. 404.6041. Anal. Calcd. for $C_{88}H_{85}B_2FeN_6O_5Zn$•$H_2O$: C, 72.02; H, 5.98; N, 5.73. Found: C, 71.81; H, 5.69; N, 6.15 %.

Synthesis of {L[$Zn^{II}(\mu$–OAc)$_2Zn^{II}$]}BPh_4 (3)

ACCEPTED MANUSCRIPT

NEt_3 (0.0880 g, 0.869 mmol) and $Zn(OAc)_2 \cdot 2H_2O$ (0.191 g, 0.872 mmol) were added to a solution of 2,6-*bis*{[*bis*(2-pyridylmethyl)amino]methyl}-4-*t*-butylphenol (**1**) (0.250 g, 0.436 mmol) in MeOH (10.0 mL) at 50 ^oC. The resulting solution was refluxed for 1 hour after which $NaBPh_4$ (0.298 g, 0.870 mmol) was added. Upon cooling the reaction mixture, the product precipitated out as an yellow solid. The precipitate was isolated by filtration and vacuum dried to obtain the product as an yellow solid (**3**) (0.315 g, 63 %). ^1H NMR (DMSO-d_6, 400 MHz, 25 ^oC): δ 8.72 (d, 2H, $^3J_{HH}$ = 5 Hz, $C_5\underline{H}_4N$), 8.16 (d, 2H, $^3J_{HH}$ = 5 Hz, $C_5\underline{H}_4N$'), 8.01 (dt, 2H, $^3J_{HH}$ = 8 Hz, $^4J_{HH}$ = 2 Hz, $C_5\underline{H}_4N$), 7.62 (d, 2H, $^3J_{HH}$ = 8 Hz, $C_5\underline{H}_4N$), 7.52 (t, 2H, $^3J_{HH}$ = 6 Hz, $C_5\underline{H}_4N$), 7.33 (t, 2H, $^3J_{HH}$ = 7 Hz, $C_5\underline{H}_4N$'), 7.18 (broad, 8H, $B(C_6\underline{H}_5)$), 7.08 (t, 2H, $^3J_{HH}$ = 6 Hz, $C_5\underline{H}_4N$'), 6.91 (t, 8H, $^3J_{HH}$ = 8 Hz, $B(C_6\underline{H}_5)$), 6.78 (t, 4H, $^3J_{HH}$ = 8 Hz, $B(C_6\underline{H}_5)$), 6.57 (s, 2H, $C_6\underline{H}_2$), 6.41 (d, 2H, $^3J_{HH}$ = 8 Hz, $C_5\underline{H}_4N$'), 4.37 (d, 2H, $^2J_{HH}$ = 15 Hz, $C\underline{H}_2$), 4.04 (d, 2H, $^2J_{HH}$ = 15 Hz, $C\underline{H}_2$), 3.77 (d, 2H, $^2J_{HH}$ = 11 Hz, $C\underline{H}_2$), 3.51 (d, 2H, $^2J_{HH}$ = 16 Hz, $C\underline{H}_2$), 3.27 (d, 2H, $^2J_{HH}$ = 15 Hz, $C\underline{H}_2$), 3.23 (d, 2H, $^2J_{HH}$ = 11 Hz, $C\underline{H}_2$), 1.99 (s, 6H, $C\underline{H}_3COO$) 1.11 (s, 9H, $C(C\underline{H}_3)_3$). ^{13}C {^1H} NMR (CH_3CN-d_3, 125 MHz, 25 ^oC): δ 179.69 ($2CH_3\underline{C}OO$), 165.81 ($2\underline{C}_5H_4N$), 165.42 ($2\underline{C}_5H_4N$'), 156.8 ($\underline{C}_6H_2$), 156.1 ($2\underline{C}_5H_4N$), 149.1 ($2\underline{C}_5H_4N$'), 147.6 ($2\underline{C}_5H_4N$), 140.8 ($2\underline{C}_5H_4N$'), 138.9 ($2\underline{C}_5H_4N$), 137.2 ($B(4\underline{C}_6H_5)$), 128.7 ($2\underline{C}_5H_4N$'), 127.0 ($B(8\underline{C}_6H_5)$), 126.98 ($B(8\underline{C}_6H_5)$), 125.6 ($2\underline{C}_6H_2$), 125.7 ($2\underline{C}_5H_4N$), 124.23 ($2\underline{C}_6H_2$), 124.0 ($2\underline{C}_5H_4N$'), 123.2 ($B(4\underline{C}_6H_5)$), 122.4 ($\underline{C}_6H_2$), 61.4 ($2\underline{C}H_2$), 61.1 ($2\underline{C}H_2$), 59.0 ($2\underline{C}H_2$), 48.4 ($\underline{C}(CH_3)_3$), 32.4 ($C(\underline{C}H_3)_3$), 25.4 ($2\underline{C}H_3COO$). IR data (KBr pellet) cm^{-1}: 3469 (w), 3055 (w), 3035 (w), 2962 (w), 1605 (s), 1575 (w), 1481 (m), 1425 (m), 1363 (w), 1322 (w), 1292 (w), 1220 (w), 1153 (w), 1129 (w), 1095 (w), 1050 (w), 1019 (w), 965 (w), 878 (w), 832 (w), 762 (w), 733 (w), 704 (m), 649 (w), 613 (w), 497 (w). HRMS (ES): *m/z* 821.1997 $[M–BPh_4]^+$, Calcd. 821.1991. Anal. Calcd. for $C_{64}H_{65}Zn_2BN_6O_5$: C, 67.44; H, 5.75; N, 7.37. Found: C, 67.28; H, 5.37; N, 7.79 %.

ACCEPTED MANUSCRIPT

Synthesis of {L[$Ni^{II}(\mu$–$OAc)_2Ni^{II}$]}BPh_4 (4)

NEt_3 (0.0880 g, 0.869 mmol) and $Ni(OAc)_2$•$4H_2O$ (0.216 g, 0.868 mmol) were added to a solution of 2,6-*bis*{[*bis*(2-pyridylmethyl)amino]methyl}-4-*t*-butylphenol (**1**) (0.250 g, 0.436 mmol) in MeOH (10.0 mL) at 50 ^oC. The resulting solution was refluxed for 1 hour after which $NaBPh_4$ (0.298 g, 0.870 mmol) was added. Upon cooling the reaction mixture, the product precipitated out as an yellow solid. The precipitate was isolated by filtration and vacuum dried to obtain the product as an yellow solid (**3**) (0.210 g, 43 %). IR data (KBr pellet) cm^{-1}: 3444 (w), 3055 (w), 2963 (w), 2363 (w), 1604 (s), 1482 (m), 1424 (m), 1363 (w), 1323 (w), 1289 (w), 1220 (w), 1153 (w), 1121 (w), 1049 (w), 1021 (w), 878 (w), 833 (w), 753 (w), 733 (w), 704 (m), 661 (w), 613 (w), 470 (w). HRMS (ES): *m/z* 805.2154 [M–BPh_4]$^+$, Calcd. 805.2153. Anal. Calcd. for $C_{64}H_{65}Ni_2BN_6O_5$: C, 68.24; H, 5.82; N, 7.46. Found: C, 67.99; H, 5.57; N, 7.05 %.

General procedure for spectrophotometric titration

6.0×10^{-4} M solution of **2** and 1.3×10^{-4} M (**3**/**4**) in CH_3CN/H_2O (1:1 *v/v*) with the ionic strength of 0.1 M KCl was titrated with 0.1 M NaOH solution and change in the position of λ_{max} was observed with the change in pH of the solution.

General procedure for phosphoester hydrolysis

By using a UV 3600 Shimadzu spectrophotometer increase in the concentration of the product 2,4-dinitrophenolate (BNP), was monitored at 25 ºC by UV-vis spectroscopy at 400 nm in quartz cuvettes. The kinetics measurements were done in CH_3CN:H_2O (*v/v* 1:1). For the study of the pH dependence, substrate and complex concentrations were 0.002 M and 3.75×10^{-4} M (**2**/**3**) and 0.05×10^{-3} M (**4**) respectively. The ionic strength and pH were kept constant by using total concentrations of 0.1 M $NaClO_4$ and 0.05 M buffer MES (2-(*N*-

ACCEPTED MANUSCRIPT

morpholino)ethanesulfonic acid) (pH 5.5 to 6.5), HEPES (4-(2-hydroxyethyl)-1-piperazineethanesulfonic acid) (7.0 to 8.0), CHES (*N*-Cyclohexyl-2-aminoethanesulfonic acid) (8.5 to 9.0) and CAPS (*N*-cyclohexyl-3-aminopropanesulfonic acid) (9.5 to 10.5). The pH of the buffer was adjusted in standard solutions using a calibrated pH meter. Each cuvette was prepared by successive addition of 62.5 μL of a 0.080 M standard solution of *bis*(2,4-dinitrophenyl)phosphate (2,4-BDNPP) in CH_3CN/H_2O (*v/v*1:1), 1250 μL of a 0.1 M buffer solution and 1062.5 μL of CH_3CN for **2** and **3** and 1170.5 μL of CH_3CN for **4**. After mixing, the background absorption was measured. Then 125 μL of a 0.0075 M standard solution of the complex (**2**/**3**) and 17 μL of a 0.0075 M standard solution in case of complex **4** in CH_3CN were added and the increase in absorption overtime was measured at 400 nm. The initial rates were calculated by fitting a linear line to the curve corresponding to absorbance for 15 minutes for **2** and **3** and absorbance < 5 % for **4**. The total concentration of phenol from the absorption of the phenolate at 400 nm was calculated from the molar extinction coefficient ε of BNP (12100 $M^{-1}cm^{-1}$).

For the study of dependence of substrate concentration on the initial rate, varying volume of stock solution of 2,4-*bis*-dinitrophenyl phosphate (0.08 M) was added to the cuvette to give a total concentration of 0.5–4.0 mM, while the complex concentration was kept constant at 0.05 mM. Kinetic measurements were done using Michaelis-Menten equation and the results were evaluated from Lineweaver-Burk plots.

Mass Spectrometry

General procedure

The molecular weight of the monoaquated and dihydroxo species, $\{L[(H_2O)Zn^{II}(\mu\text{–}OH)Fe^{III}(OH)]\}^{2+}$ (**2C**), $\{L[(H_2O)Zn^{II}(\mu\text{–}OH)Zn^{II}(OH)]\}^{+}$ (**3C**), the trihydroxo species,

ACCEPTED MANUSCRIPT

{L[(HO)Zn^{II}(μ–OH)Fe^{III}(OH)]}$^{+}$ (**2D**), {L[(HO)M^1(μ–OH)M^2(OH)]} [M^1 = M^2 = Zn (**3D**), Ni (**4D**)] and the metal bound *bis*(2,4−dinitrophenyl)phosphate (2,4−BDNPP) species {L[(R_2PO_4)Zn^{II}(μ–OH)Fe^{III}(OH)]}$^{+}$ (**2E**), {L[Zn^{II}(μ–OH)(μ–RPO_4)Fe^{III}]}$^{+}$ (**2F**), and {L[Zn^{II}(μ–OH)(μ–RPO_4)Zn^{II}]} (**3F**), of the proposed mechanistic cycle were characterized by direct-injection electrospray mass spectrometry (DIESI-MS) studies performed on a BRUKER maxis impact mass spectrometer. The measurements were obtained in positive ion detection modes on an ion trap mass spectrometer with an ESI source.

General procedure for the direct ionization ESI-MS detection of the (**2C**), (**3C**), (**2D**), (**3D**) and (**4D**)

The **2**, **3** and **4** complexes were dissolved in CH_3CN/H_2O (*v/v* 1:1) mixed medium (1.00 mL) at room temperature and was further diluted with CH_3CN/H_2O (*v/v* 1:1) (5.00 mL). An aliquot of the sample solution was directly injected the ESI-MS to obtain the mass spectrometric data.

General procedure for the direct ionization ESI-MS detection of the (**2E**), (**2F**) and (**3F**)

The data was collected under kinetic conditions. Each vial was prepared by successive addition of 1062.5 μL of CH_3CN, 62.5 μL of a 0.080 M standard solution of *bis*(2,4-dinitrophenyl)phosphate (2,4-BDNPP) in CH_3CN:H_2O (*v/v* 1:1), 1250 μL of a 0.1 M buffer solution containing 0.2 M $NaClO_4$ (pH = 6.5) and 125 μL of a 0.0075 M standard solution of the complex (**2**/**3**) in CH_3CN was added. The reaction mixture was then diluted with CH_3CN:H_2O (*v/v* 1:1) (5.00 mL) and an aliquot of the sample solution was directly injected into the ESI-MS to obtain the mass spectrometric data.

ACCEPTED MANUSCRIPT

Supporting Information

^{1}H NMR, ^{13}C{^{1}H} NMR, IR spectra, HRMS and elemental analysis data of 2,6-*bis*{[*bis*(2-pyridylmethyl)amino]methyl}-4-*t*-butylphenol, (HL) (**1**), the metal complexes **2**, **3** and **4**. CIF file giving X-ray crystallographic data; variable-temperature magnetic susceptibility and effective magnetic moment plots for **2** and **4** complex, electronic spectroscopic data for **2**, **3** and **4** complexes; spectrophotometric titration data of complexes **3** and **4** including catalysis data and mass experiments of the catalysis intermediates (**2C**), (**2D**), (**2E**), (**2F**), (**3C**), (**3D**), (**3F**), and (**4D**) can be found in the journal webpage. This material is available free of charge *via* journal webpage.

ACCEPTED MANUSCRIPT

ACCEPTED MANUSCRIPT

Abbreviations

2,4−BDNPP	*bis*(2,4−dinitrophenyl)phosphate
PAP	purple acid phosphatase
HL	2,6-*bis*{[*bis*(2-pyridylmethyl)amino]methyl}-4-*t*-butylphenol
LMCT	ligand-to-metal charge transfer
DESI-MS	direct-injection electrospray mass spectrometry
DMSO	dimethylsulfoxide
MES	2-(*N*-morpholino)ethanesulfonic acid
HEPES	4-(2-hydroxyethyl)-1-piperazineethanesulfonic acid
CHES	*N*-Cyclohexyl-2-aminoethanesulfonic acid
CAPS	*N*-cyclohexyl-3-aminopropanesulfonic acid
ICPAES	Inductively Coupled Plasma Atomic Emission Spectroscopy
PPMS	Physical Property Measurement System
HBPMP	2,6-*bis*[(*bis*(2-pyridylmethyl)amino)methyl)]-4-methylphenol
HBPMOP	2,6-*bis*[{*bis*(2-pyridylmethyl)amino}methyl]-4-methoxyphenol
BMMHP	2-{[*bis*(2-methoxyethyl)-amino]methyl}-6-{[(2-hydroxybenzyl)(2-pyridylmethyl)amino]-methyl}-4-methylphenol
IPCPMP	2-(*N*-isopropyl-*N*-((2-pyridyl)methyl)aminomethyl)-6-(*N*-(carboxylmethyl)-*N*-((2-pyridyl)methyl)aminomethyl)-4-methylphenol
HL^1	2-{[*bis*(2-methylpyridyl)-amino]methyl}-6-{[((1-methylimidazol-2-yl)methyl)(2-pyridylmethyl)amino]methyl}-4-t-butylphenol
$H_2BPBPMP$	2-*bis*[{(2-pyridylmethyl)-aminomethyl}-6-{(2-hydroxybenzyl)(2-pyridylmethyl)}-aminomethyl]-4-methylphenol
H_3L^2	2,6-bis{[(2-hydroxybenzyl)(2-pyridylmethyl)amino]methyl]-4-methylphenol)
HTPDP	1,3-*bis*(*bis*-pyridin-2-ylmethylamino)propan-2-ol
CH_3L^3	2-(((2-methoxyethyl)(pyridine-2-ylmethyl)-amino)methyl)-4-methyl-6-(((pyridin-2-ylmethyl)(4-vinylbenzyl)-amino)methyl)phenol
H_3L^4	2,6-*bis*((hydroxyethyl)(methoxyethyl)-aminomethyl)-4-methylphenol
AA	acetohydroxamate anion
tmen	N,N,N¢,N¢-tetramethylethylenediamine
L^5	2-[*N*-*bis*-(2-pyridylmethyl)aminomethyl]-4-methyl-6-[*N*-(2-pyridylmethyl)aminomethyl]phenolate)
L^{Cl}-OH	2,6-*bis*[*bis*(2-pyridylmethyl)aminomethyl]-4-chlorophenol
L^6	2-[*N*-*bis*-(2-pyridylmethyl)aminomethyl]-4-methyl-6-[*N*-(2-pyridylmethyl)aminomethyl]phenolate)
BCIMP	2,6-bis[N-(N-(carboxylmethyl)-N-((1-methylimidazolyl) methyl)amine)methyl]-4-methylphenolate

ACCEPTED MANUSCRIPT

Acknowledgement

We thank the Department of Science and Technology (EMR/2014/000254), New Delhi, India, for financial support of this research. We gratefully acknowledge the Single Crystal X-ray diffraction Facility, Department of Chemistry, IIT Bombay, Mumbai, India, for the crystallographic characterization data and central facility, Industrial Research and Consultancy Center (IRCC), IIT Bombay for Physical Property Measurement System (PPMS). C.P. thanks UGC, New Delhi, India, for research fellowships. D.K and M.K.G. thank CSIR, New Delhi, India, for research fellowships.

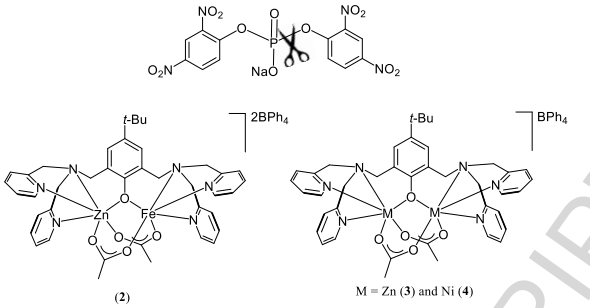
ACCEPTED MANUSCRIPT

ACCEPTED MANUSCRIPT

Graphics for Table of Contents

Heterodinuclear Zn(II)−Fe(III) and Homodinuclear M(II)−M(II) [M = Zn and Ni] Complexes of a Bicompartmental [N_6O] Ligand as Synthetic Mimics of the Hydrolase Family of Enzymes

*Chandni Pathak, Dharmendra Kumar, Manoj Kumar Gangwar, Darshan Mhatre, Thierry Roisnel, and Prasenjit Ghosh**



A heterodinuclear mixed valence zinc−iron and two homodinuclear zinc–zinc and nickel–nickel type complexes supported over a symmetrical nitrogen and oxygen donors bearing ligand serve as small molecule functional mimics of the hydrolase family of enzymes.

ACCEPTED MANUSCRIPT

ACCEPTED MANUSCRIPT

References

[1] M.L. Zastrow, V.L. Pecoraro, Biochemistry, vol. 53, American Chemical Society, 2014, pp. 957-978.

[2] J.L. Boer, S.B. Mulrooney, R.P. Hausinger, Archives of Biochemistry and Biophysics, vol. 544, 2014, pp. 142-152.

[3] M. Can, F.A. Armstrong, S.W. Ragsdale, Chemical Reviews, vol. 114, American Chemical Society, 2014, pp. 4149-4174.

[4] R. Hille, J. Hall, P. Basu, Chemical Reviews, vol. 114, American Chemical Society, 2014, pp. 3963-4038.

[5] Y.-W. Lin, Coordination Chemistry Reviews, vol. 336, 2017, pp. 1-27.

[6] J.P. Collman, Inorganic Chemistry, vol. 36, American Chemical Society, 1997, pp. 5145-5155.

[7] A. Stassinopoulos, S. Mukerjee, J.P. Caradonna, Mechanistic Bioinorganic Chemistry, vol. 246, Advances in Chemistry, American Chemical Society, 1996, pp. 83-120.

[8] E.I. Solomon, D.E. Heppner, E.M. Johnston, J.W. Ginsbach, J. Cirera, M. Qayyum, M.T. Kieber-Emmons, C.H. Kjaergaard, R.G. Hadt, L. Tian, Chemical Reviews, vol. 114, American Chemical Society, 2014, pp. 3659-3853.

[9] P.E.M. Siegbahn, M.R.A. Blomberg, Chemical Reviews, vol. 110, American Chemical Society, 2010, pp. 7040-7061.

[10] J. Liu, S. Chakraborty, P. Hosseinzadeh, Y. Yu, S. Tian, I. Petrik, A. Bhagi, Y. Lu, Chemical Reviews, vol. 114, American Chemical Society, 2014, pp. 4366-4469.

[11] D. Schilter, J.M. Camara, M.T. Huynh, S. Hammes-Schiffer, T.B. Rauchfuss, Chemical Reviews, vol. 116, American Chemical Society, 2016, pp. 8693-8749.

ACCEPTED MANUSCRIPT

[12] V.C.C. Wang, S. Maji, P.P.Y. Chen, H.K. Lee, S.S.F. Yu, S.I. Chan, Chemical Reviews, vol. 117, American Chemical Society, 2017, pp. 8574-8621.

[13] G. Schenk, N. Mitic, L.R. Gahan, D.L. Ollis, R.P. McGeary, L.W. Guddat, Acc. Chem. Res., vol. 45, American Chemical Society, 2012, pp. 1593-1603.

[14] D.E. Wilcox, Chemical Reviews, vol. 96, American Chemical Society, 1996, pp. 2435-2458.

[15] C. Liu, L. Wang, Dalton Transactions, The Royal Society of Chemistry, 2009, pp. 227-239.

[16] G. Schenk, N. Mitić, G.R. Hanson, P. Comba, Coordination Chemistry Reviews, vol. 257, 2013, pp. 473-482.

[17] L.R. Gahan, S.J. Smith, A. Neves, G. Schenk, European Journal of Inorganic Chemistry, vol. 2009, WILEY-VCH Verlag, 2009, pp. 2745-2758.

[18] E. Ghanem, Y. Li, C. Xu, F.M. Raushel, Biochemistry, vol. 46, American Chemical Society, 2007, pp. 9032-9040.

[19] F. Meyer, European Journal of Inorganic Chemistry, vol. 2006, WILEY-VCH Verlag, 2006, pp. 3789-3800.

[20] G. Parkin, Chemical Reviews, vol. 104, American Chemical Society, 2004, pp. 699-768.

[21] N. Sträter, B. Jasper, M. Scholte, B. Krebs, A.P. Duff, D.B. Langley, R. Han, B.A. Averill, H.C. Freeman, J.M. Guss, Journal of Molecular Biology, vol. 351, 2005, pp. 233-246.

[22] G. Schenk, L.R. Gahan, L.E. Carrington, N. Mitić, M. Valizadeh, S.E. Hamilton, J. de Jersey, L.W. Guddat, Proceedings of the National Academy of Sciences of the United States of America, vol. 102, 2005, pp. 273-278.

[23] L.W. Guddat, A.S. McAlpine, D. Hume, S. Hamilton, J. de Jersey, J.L. Martin, Structure, vol. 7, 1999, pp. 757-767.

ACCEPTED MANUSCRIPT

[24] Y. Lindqvist, E. Johansson, H. Kaija, P. Vihko, G. Schneider, Journal of Molecular Biology, vol. 291, 1999, pp. 135-147.

[25] J. Uppenberg, F. Lindqvist, C. Svensson, B. Ek-Rylander, G. Andersson, Journal of Molecular Biology, vol. 290, 1999, pp. 201-211.

[26] T. Klabunde, N. Sträter, R. Fröhlich, H. Witzel, B. Krebs, Journal of Molecular Biology, vol. 259, 1996, pp. 737-748.

[27] N. Strater, T. Klabunde, P. Tucker, H. Witzel, B. Krebs, Science, vol. 268, 1995, pp. 1489.

[28] G. Schenk, M.L.J. Korsinczky, D.A. Hume, S. Hamilton, J. DeJersey, Gene, vol. 255, 2000, pp. 419-424.

[29] S.K. Smoukov, L. Quaroni, X. Wang, P.E. Doan, B.M. Hoffman, L. Que, Journal of the American Chemical Society, vol. 124, American Chemical Society, 2002, pp. 2595-2603.

[30] B.A. Averill, J.C. Davis, S. Burman, T. Zirino, J. Sanders-Loehr, T.M. Loehr, J.T. Sage, P.G. Debrunner, Journal of the American Chemical Society, vol. 109, American Chemical Society, 1987, pp. 3760-3767.

[31] B. Das, H. Daver, M. Pyrkosz-Bulska, E. Persch, S.K. Barman, R. Mukherjee, E. Gumienna-Kontecka, M. Jarenmark, F. Himo, E. Nordlander, Journal of Inorganic Biochemistry, vol. 132, 2014, pp. 6-17.

[32] M.M. Benning, J.M. Kuo, F.M. Raushel, H.M. Holden, Biochemistry, vol. 33, American Chemical Society, 1994, pp. 15001-15007.

[33] G. Schenk, I. Mateen, T.-K. Ng, M.M. Pedroso, N. Mitic, M. Jafelicci, R.F.C. Marques, L.R. Gahan, D.L. Ollis, Coord. Chem. Rev., vol. 317, Elsevier B.V., 2016, pp. 122-131.

[34] E. Ghanem, F.M. Raushel, Toxicol. Appl. Pharmacol., vol. 207, Elsevier, 2005, pp. S459-S470.

ACCEPTED MANUSCRIPT

[35] J.K. Grimsley, J.M. Scholtz, C.N. Pace, J.R. Wild, Biochemistry, vol. 36, American Chemical Society, 1997, pp. 14366-14374.

[36] F.M. Raushel, Curr. Opin. Microbiol., vol. 5, Elsevier Science Ltd., 2002, pp. 288-295.

[37] N. Sethunathan, T. Yoshida, Can. J. Microbiol., vol. 19, 1973, pp. 873-875.

[38] D.M. Munnecke, Appl. Environ. Microbiol., vol. 32, 1976, pp. 7-13.

[39] J.J. Brown, L.R. Gahan, A. Schoffler, E.H. Krenske, G. Schenk, J. Inorg. Biochem., vol. 162, Elsevier, 2016, pp. 356-365.

[40] H. Arora, S.K. Barman, F. Lloret, R. Mukherjee, Inorganic Chemistry, vol. 51, American Chemical Society, 2012, pp. 5539-5553.

[41] P. Comba, L.R. Gahan, V. Mereacre, G.R. Hanson, A.K. Powell, G. Schenk, M. Zajaczkowski-Fischer, Inorganic Chemistry, vol. 51, American Chemical Society, 2012, pp. 12195-12209.

[42] F. Heims, V. Mereacre, A. Ciancetta, S. Mebs, A.K. Powell, C. Greco, K. Ray, Eur. J. Inorg. Chem., vol. 2012, Wiley-VCH Verlag GmbH & Co. KGaA, 2012, pp. 4565-4569, S4565/4561-S4565/4569.

[43] S. Albedyhl, D. Schnieders, A. Jancso, T. Gajda, B. Krebs, Eur. J. Inorg. Chem., Wiley-VCH Verlag GmbH, 2002, pp. 1400-1409.

[44] S. Albedyhl, M.T. Averbuch-Pouchot, C. Belle, B. Krebs, J.L. Pierre, E. Saint-Aman, S. Torelli, Eur. J. Inorg. Chem., Wiley-VCH Verlag GmbH, 2001, pp. 1457-1464.

[45] M. Ghiladi, C. J. McKenzie, A. Meier, A. K. Powell, J. Ulstrup, S. Wocadlo, Journal of the Chemical Society, Dalton Transactions, The Royal Society of Chemistry, 1997, pp. 4011-4018.

[46] A.S. Borovik, V. Papaefthymiou, L.F. Taylor, O.P. Anderson, L. Que, Jr., J. Am. Chem. Soc., vol. 111, 1989, pp. 6183-6195.

ACCEPTED MANUSCRIPT

[47] R.M. Buchanan, M.S. Mashuta, K.J. Oberhausen, J.F. Richardson, Q. Li, D.N. Hendrickson, J. Am. Chem. Soc., vol. 111, 1989, pp. 4497-4498.

[48] M. Suzuki, H. Oshio, A. Uehara, K. Endo, M. Yanaga, S. Kida, K. Saito, Bull. Chem. Soc. Jpn., vol. 61, 1988, pp. 3907-3913.

[49] M. Suzuki, H. Kanatomi, I. Murase, Chemistry Letters, vol. 10, The Chemical Society of Japan, 1981, pp. 1745-1748.

[50] S. Bosch, P. Comba, L.R. Gahan, G. Schenk, J. Inorg. Biochem., vol. 162, Elsevier, 2016, pp. 343-355.

[51] P.V. Bernhardt, S. Bosch, P. Comba, L.R. Gahan, G.R. Hanson, V. Mereacre, C.J. Noble, A.K. Powell, G. Schenk, H. Wadepohl, Inorg. Chem., vol. 54, American Chemical Society, 2015, pp. 7249-7263.

[52] A.E. Roberts, G. Schenk, L.R. Gahan, Eur. J. Inorg. Chem., vol. 2015, Wiley-VCH Verlag GmbH & Co. KGaA, 2015, pp. 3076-3086.

[53] M. Carboni, M. Clemancey, F. Molton, J. Pecaut, C. Lebrun, L. Dubois, G. Blondin, J.M. Latour, Inorg. Chem., vol. 51, American Chemical Society, 2012, pp. 10447-10460.

[54] F.R. Xavier, A.J. Bortoluzzi, A. Neves, Chem. Biodiversity, vol. 9, Verlag Helvetica Chimica Acta, 2012, pp. 1794-1805.

[55] E. Lambert, B. Chabut, S. Chardon-Noblat, A. Deronzier, G. Chottard, A. Bousseksou, J.-P. Tuchagues, J. Laugier, M. Bardet, J.-M. Latour, Journal of the American Chemical Society, vol. 119, American Chemical Society, 1997, pp. 9424-9437.

[56] A. Neves, M. Aires de Brito, V. Drago, K. Griesar, W. Haase, Inorganica Chimica Acta, vol. 237, 1995, pp. 131-135.

[57] E. Bernard, W. Moneta, J. Laugier, S. Chardon-Noblat, A. Deronzier, J.-P. Tuchagues, J.-M. Latour, Angewandte Chemie International Edition in English, vol. 33, Hüthig & Wepf Verlag, 1994, pp. 887-889.

ACCEPTED MANUSCRIPT

[58] L.L. Mendes, D. Englert, C. Fernandes, L.R. Gahan, G. Schenk, A. Horn, Dalton Transactions, vol. 45, The Royal Society of Chemistry, 2016, pp. 18510-18521.

[59] S. Bosch, P. Comba, L.R. Gahan, G. Schenk, Inorganic Chemistry, vol. 53, American Chemical Society, 2014, pp. 9036-9051.

[60] K. Selmeczi, C. Michel, A. Milet, I. Gautier-Luneau, C. Philouze, J.-L. Pierre, D. Schnieders, A. Rompel, C. Belle, Chemistry – A European Journal, vol. 13, WILEY-VCH Verlag, 2007, pp. 9093-9106.

[61] E. Kinoshita, M. Takahashi, H. Takeda, M. Shiro, T. Koike, Dalton Transactions, The Royal Society of Chemistry, 2004, pp. 1189-1193.

[62] B. de Souza, G.L. Kreft, T. Bortolotto, H. Terenzi, A.J. Bortoluzzi, E.E. Castellano, R.A. Peralta, J.B. Domingos, A. Neves, Inorganic Chemistry, vol. 52, American Chemical Society, 2013, pp. 3594-3596.

[63] S.J. Smith, R.A. Peralta, R. Jovito, A. Horn, A.J. Bortoluzzi, C.J. Noble, G.R. Hanson, R. Stranger, V. Jayaratne, G. Cavigliasso, L.R. Gahan, G. Schenk, O.R. Nascimento, A. Cavalett, T. Bortolotto, G. Razzera, H. Terenzi, A. Neves, M.J. Riley, Inorganic Chemistry, vol. 51, American Chemical Society, 2012, pp. 2065-2078.

[64] C. Piovezan, R. Jovito, A.J. Bortoluzzi, H. Terenzi, F.L. Fischer, P.C. Severino, C.T. Pich, G.G. Azzolini, R.A. Peralta, L.M. Rossi, A. Neves, Inorganic Chemistry, vol. 49, American Chemical Society, 2010, pp. 2580-2582.

[65] F.R. Xavier, A. Neves, A. Casellato, R.A. Peralta, A.J. Bortoluzzi, B. Szpoganicz, P.C. Severino, H. Terenzi, Z. Tomkowicz, S. Ostrovsky, W. Haase, A. Ozarowski, J. Krzystek, J. Telser, G. Schenk, L.R. Gahan, Inorganic Chemistry, vol. 48, American Chemical Society, 2009, pp. 7905-7921.

ACCEPTED MANUSCRIPT

[66] A. Neves, M. Lanznaster, A.J. Bortoluzzi, R.A. Peralta, A. Casellato, E.E. Castellano, P. Herrald, M.J. Riley, G. Schenk, Journal of the American Chemical Society, vol. 129, American Chemical Society, 2007, pp. 7486-7487.

[67] M. Lanznaster, A. Neves, A.J. Bortoluzzi, V.V.E. Aires, B. Szpoganicz, H. Terenzi, P.C. Severino, J.M. Fuller, S.C. Drew, L.R. Gahan, G.R. Hanson, M.J. Riley, G. Schenk, JBIC Journal of Biological Inorganic Chemistry, vol. 10, 2005, pp. 319-332.

[68] S.C. Batista, A. Neves, A.J. Bortoluzzi, I. Vencato, R.A. Peralta, B. Szpoganicz, V.V.E. Aires, H. Terenzi, P.C. Severino, Inorganic Chemistry Communications, vol. 6, 2003, pp. 1161-1165.

[69] M. Lanznaster, A. Neves, A.J. Bortoluzzi, B. Szpoganicz, E. Schwingel, Inorganic Chemistry, vol. 41, American Chemical Society, 2002, pp. 5641-5643.

[70] P. Karsten, A. Neves, A.J. Bortoluzzi, M. Lanznaster, V. Drago, Inorganic Chemistry, vol. 41, American Chemical Society, 2002, pp. 4624-4626.

[71] C. Belle, I. Gautier-Luneau, L. Karmazin, J.-L. Pierre, S. Albedyhl, B. Krebs, M. Bonin, Eur. J. Inorg. Chem., Wiley-VCH Verlag GmbH & Co. KGaA, 2002, pp. 3087-3090.

[72] C. Belle, I. Gautier-Luneau, G. Gellon, J.-L. Pierre, I. Morgenstern-Badarau, E. Saint-Aman, Journal of the Chemical Society, Dalton Transactions, The Royal Society of Chemistry, 1997, pp. 3543-3546.

[73] M. Carboni, M. Clémancey, F. Molton, J. Pécaut, C. Lebrun, L. Dubois, G. Blondin, J.M. Latour, Inorganic Chemistry, vol. 51, American Chemical Society, 2012, pp. 10447-10460.

[74] B. Das, H. Daver, A. Singh, R. Singh, M. Haukka, S. Demeshko, F. Meyer, G. Lisensky, M. Jarenmark, F. Himo, E. Nordlander, European Journal of Inorganic Chemistry, vol. 2014, WILEY-VCH Verlag, 2014, pp. 2204-2212.

ACCEPTED MANUSCRIPT

[75] L.J. Daumann, L. Marty, G. Schenk, L.R. Gahan, Dalton Transactions, vol. 42, The Royal Society of Chemistry, 2013, pp. 9574-9584.

[76] M. Jarenmark, M. Haukka, S. Demeshko, F. Tuczek, L. Zuppiroli, F. Meyer, E. Nordlander, Inorganic Chemistry, vol. 50, American Chemical Society, 2011, pp. 3866-3887.

[77] M. Jarenmark, E. Csapo, J. Singh, S. Wockel, E. Farkas, F. Meyer, M. Haukka, E. Nordlander, Dalton Transactions, vol. 39, The Royal Society of Chemistry, 2010, pp. 8183-8194.

[78] M. Jarenmark, H. Carlsson, V.M. Trukhan, M. Haukka, S.E. Canton, M. Walczak, W. Fullagar, V. Sundstroem, E. Nordlander, Inorg. Chem. Commun., vol. 13, Elsevier B.V., 2010, pp. 334-337.

[79] M. Jarenmark, S. Kappen, M. Haukka, E. Nordlander, Dalton Trans., Royal Society of Chemistry, 2008, pp. 993-996.

[80] T.P. Camargo, F.F. Maia, C. Chaves, B. de Souza, A.J. Bortoluzzi, N. Castilho, T. Bortolotto, H. Terenzi, E.E. Castellano, W. Haase, Z. Tomkowicz, R.A. Peralta, A. Neves, Journal of Inorganic Biochemistry, vol. 146, 2015, pp. 77-88.

[81] L.J. Daumann, K.E. Dalle, G. Schenk, R.P. McGeary, P.V. Bernhardt, D.L. Ollis, L.R. Gahan, Dalton Transactions, vol. 41, The Royal Society of Chemistry, 2012, pp. 1695-1708.

[82] J. Martinez-Sanchez, R. Bastida, A. Macias, H. Adams, D.E. Fenton, P. Perez-Lourido, L. Valencia, Polyhedron, vol. 29, Elsevier Ltd., 2010, pp. 2651-2656.

[83] R.R. Buchholz, M.E. Etienne, A. Dorgelo, R.E. Mirams, S.J. Smith, S.Y. Chow, L.R. Hanton, G.B. Jameson, G. Schenk, L.R. Gahan, Dalton Transactions, The Royal Society of Chemistry, 2008, pp. 6045-6054.

[84] A. Neves, M.A. de Brito, I. Vencato, V. Drago, K. Griesar, W. Haase, Inorganic Chemistry, vol. 35, American Chemical Society, 1996, pp. 2360-2368.

ACCEPTED MANUSCRIPT

[85] B. Krebs, K. Schepers, B. Bremer, G. Henkel, E. Althaus, W. Mueller-Warmuth, K. Griesar, W. Haase, Inorganic Chemistry, vol. 33, American Chemical Society, 1994, pp. 1907-1914.

[86] S. Mandal, V. Balamurugan, F. Lloret, R. Mukherjee, Inorganic Chemistry, vol. 48, American Chemical Society, 2009, pp. 7544-7556.

[87] T. Koga, H. Furutachi, T. Nakamura, N. Fukita, M. Ohba, K. Takahashi, H. Ōkawa, Inorganic Chemistry, vol. 37, American Chemical Society, 1998, pp. 989-996.

[88] Y.-w. Ren, J.-x. Lu, B.-w. Cai, D.-b. Shi, H.-f. Jiang, J. Chen, D. Zheng, B. Liu, Dalton Transactions, vol. 40, The Royal Society of Chemistry, 2011, pp. 1372-1381.

[89] V.K. Bhardwaj, A. Singh, Inorganic Chemistry, vol. 53, American Chemical Society, 2014, pp. 10731-10742.

[90] D. Volkmer, B. Hommerich, K. Griesar, W. Haase, B. Krebs, Inorganic Chemistry, vol. 35, American Chemical Society, 1996, pp. 3792-3803.

[91] M.K. Panda, M.M. Shaikh, R.J. Butcher, P. Ghosh, Inorg. Chim. Acta, vol. 372, 2011, pp. 145-151.

[92] M.K. Panda, A. John, M.M. Shaikh, P. Ghosh, Inorg. Chem., vol. 47, 2008, pp. 11847-11856.

[93] A. John, M.M. Shaikh, P. Ghosh, Dalton Trans., 2008, pp. 2815-2824.

[94] C. Pathak, S.K. Gupta, M.K. Gangwar, A.P. Prakasham, P. Ghosh, ACS Omega, vol. 2, American Chemical Society, 2017, pp. 4737-4750.

[95] M. Ghiladi, K. B. Jensen, J. Jiang, C. J. McKenzie, S. Morup, I. Sotofte, J. Ulstrup, Journal of the Chemical Society, Dalton Transactions, The Royal Society of Chemistry, 1999, pp. 2675-2681.

[96] G.G. Bozzo, K.G. Raghothama, W.C. Plaxton, Biochemical Journal, vol. 377, 2004, pp. 419.

ACCEPTED MANUSCRIPT

[97] J.B. Vincent, G.L. Olivier-Lilley, B.A. Averill, Chemical Reviews, vol. 90, American Chemical Society, 1990, pp. 1447-1467.

[98] N. Mitic, C.J. Noble, L.R. Gahan, G.R. Hanson, G. Schenk, J. Am. Chem. Soc., vol. 131, American Chemical Society, 2009, pp. 8173-8179.

[99] Y.-S. Yang, J.M. McCormick, E.I. Solomon, J. Am. Chem. Soc., vol. 119, American Chemical Society, 1997, pp. 11832-11842.

[100] S.S. Massoud, C.C. Ledet, T. Junk, S. Bosch, P. Comba, R. Herchel, J. Hosek, Z. Travnicek, R.C. Fischer, F.A. Mautner, Dalton Transactions, vol. 45, The Royal Society of Chemistry, 2016, pp. 12933-12950.

[101] A. Greatti, M. Scarpellini, R.A. Peralta, A. Casellato, A.J. Bortoluzzi, F.R. Xavier, R. Jovito, M. Aires de Brito, B. Szpoganicz, Z. Tomkowicz, M. Rams, W. Haase, A. Neves, Inorg. Chem., vol. 47, American Chemical Society, 2008, pp. 1107-1119.

[102] G.B. Deacon, R.J. Phillips, Coordination Chemistry Reviews, vol. 33, 1980, pp. 227-250.

[103] C. Selleck, D. Clayton, L.R. Gahan, N. Mitic, R.P. McGeary, M.M. Pedroso, L.W. Guddat, G. Schenk, Chem. - Eur. J., vol. 23, Wiley-VCH Verlag GmbH & Co. KGaA, 2017, pp. 4778-4781.

[104] N. Straeter, T. Klabunde, P. Tucker, H. Witzel, B. Krebs, Science (Washington, D. C.), vol. 268, American Association for the Advancement of Science, 1995, pp. 1489-1492.

[105] M.M. Benning, H. Shim, F.M. Raushel, H.M. Holden, Biochemistry, vol. 40, American Chemical Society, 2001, pp. 2712-2722.

[106] A.S. Borovik, L. Que, V. Papaefthymiou, E. Muenck, L.F. Taylor, O.P. Anderson, Journal of the American Chemical Society, vol. 110, American Chemical Society, 1988, pp. 1986-1988.

ACCEPTED MANUSCRIPT

[107] J. Martínez-Sánchez, R. Bastida, A. Macías, H. Adams, D.E. Fenton, P. Pérez-Lourido, L. Valencia, Polyhedron, vol. 29, 2010, pp. 2651-2656.

[108] H. Adams, D. Bradshaw, D.E. Fenton, Eur. J. Inorg. Chem., Wiley-VCH Verlag GmbH, 2002, pp. 535-538.

[109] M. Arnold, D.A. Brown, O. Deeg, W. Errington, W. Haase, K. Herlihy, T.J. Kemp, H. Nimir, R. Werner, Inorganic Chemistry, vol. 37, American Chemical Society, 1998, pp. 2920-2925.

[110] A. Greatti, M. Scarpellini, R.A. Peralta, A. Casellato, A.J. Bortoluzzi, F.R. Xavier, R. Jovito, M.A. de Brito, B. Szpoganicz, Z. Tomkowicz, M. Rams, W. Haase, A. Neves, Inorganic Chemistry, vol. 47, American Chemical Society, 2008, pp. 1107-1119.

[111] H. Carlsson, M. Haukka, A. Bousseksou, J.-M. Latour, E. Nordlander, Inorganic Chemistry, vol. 43, American Chemical Society, 2004, pp. 8252-8262.

[112] N.F. Chilton, R.P. Anderson, L.D. Turner, A. Soncini, K.S. Murray, Journal of Computational Chemistry, vol. 34, Wiley Subscription Services, Inc., A Wiley Company, 2013, pp. 1164-1175.

[113] The Journal of Chemical Physics, vol. 26, American Institute of Physics, 1957, pp. 1405-1406.

[114] M.B. Twitchett, G. Schenk, M.A.S. Aquino, D.T.Y. Yiu, T.-C. Lau, A.G. Sykes, Inorganic Chemistry, vol. 41, American Chemical Society, 2002, pp. 5787-5794.

[115] S.J. Smith, A. Casellato, K.S. Hadler, N. Mitić, M.J. Riley, A.J. Bortoluzzi, B. Szpoganicz, G. Schenk, A. Neves, L.R. Gahan, JBIC Journal of Biological Inorganic Chemistry, vol. 12, 2007, pp. 1207-1220.

[116] D.E.C. Ferreira, W.B. De Almeida, A. Neves, W.R. Rocha, Physical Chemistry Chemical Physics, vol. 10, The Royal Society of Chemistry, 2008, pp. 7039-7046.

ACCEPTED MANUSCRIPT

[117] C.A. Bunton, S.J. Farber, The Journal of Organic Chemistry, vol. 34, American Chemical Society, 1969, pp. 767-772.

[118] M.E. Amato, F.P. Ballistreri, A. Pappalardo, D. Sciotto, G.A. Tomaselli, R.M. Toscano, Tetrahedron, vol. 63, 2007, pp. 9751-9757.

[119] L.J. Farrugia, J. Appl. Crystallogr., vol. 45, International Union of Crystallography, 2012, pp. 849-854.

[120] G.M. Sheldrick, Acta Crystallogr., Sect. C: Struct. Chem., vol. 71, International Union of Crystallography, 2015, pp. 3-8.

ACCEPTED MANUSCRIPT